AIAA – 2017 Multi Mission Amphibian (MMA)

Undergraduate Team Design Competition

Conceptual Design

of Mi-1

Prepared by: Magnificent Idea Team

Designers: Serdar Avşar, Mehmet Soylu, Alperen Sunay, Muzaffer Toprak

Signature Page

Team Members	Signature	AIAA Number
Serdar Avşar	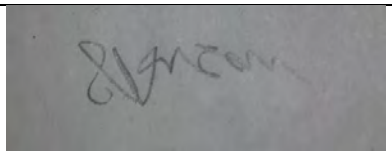	590303
Mehmet Soylu	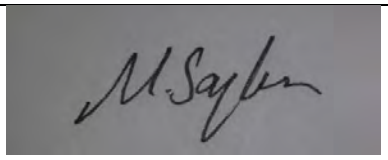	532830
Alperen Sunay	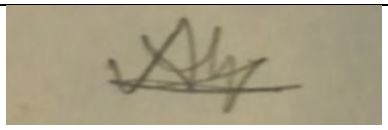	819130
Muzaffer Toprak	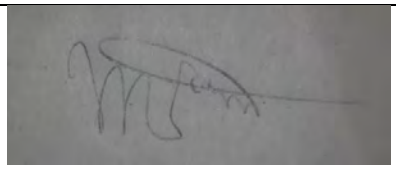	486801
Prof. Dr. Serkan Özgen (Advisor)	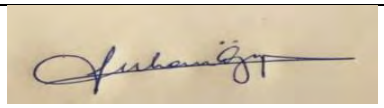	327810

Left- Serdar Avşar, Middle- Alperen Sunay, Down- Muzaffer Toprak, Right- Mehmet Soylu

Table of Contents

1 Chapter 1 – Design Overview

1.1 Introduction

The mission environment is specified as an area with small land clearance and large bodies of water. Due to the lack of a long runway, an amphibious aircraft is needed to transport people and commodities in and out of the area as well as provide the local authorities with an aerial surveillance tool.

The overall requirements prioritized efficiency, payload and endurance in passenger, cargo and surveillance missions respectively. To achieve the mandatory requirements these had to be the focus of the study so that MI-1 can be successful in every aspect of its missions

In the passenger mission, the aircraft had to be efficient while also satisfying the necessary challenging requirements of takeoff and landing distances. The aircraft also has to be easy to repair and reliable. This prevents the designers from using too much composite materials. However, a composite trade study was done nonetheless.

The cargo mission was the easiest in terms of satisfying the requirements. Thus, it did not affect the overall design process very much. The challenging part was to carry a standard container as a target requirement. It was assumed as a ship container at first. The aircraft was designed very big to satisfy this requirement. Later it was found out that the standard container was a standard aircraft container.

In the surveillance mission the challenging requirement was the endurance. The aircraft had to carry more fuel than it does in passenger and cargo missions.

1.2 Requirements

1.2.1 General Requirements:

- (M) Capable of taking off and landing from runways (dirt, grass, metal mat, gravel, asphalt & 2017 Multi-Mission Amphibian (MMA) Undergraduate Team Design Competition concrete)
- (M) Capable of taking off and landing from fresh and salt water
- (M) Minimum cruise speed of 200 knots on
- (T) Target cruise speed: 250 knots or greater
- (M) Capable of VFR and IFR flight
- (M) Capable of flight in known icing conditions
- (M) Meets applicable certification rules in FAA 14 CFR Part 25
- (M) Fuel burn per passenger at least 20% better than an existing aircraft on a similar mission length
- Economic mission of 500 nmi in a single class configuration
- (M) Engine/propulsion system assumptions documented and the use of an engine that will be in service by 2027.

(M): Mandatory Requirement

(T): Tradable Requirement

1.2.2 Passenger Mission:

- (M) Crew: 2 flight crew, 1 cabin crew member
- (M) Minimum passenger capacity: 20 at a 28” or greater seat pitch
- (T) maximum capacity of between 20 and 49 single-class seats
- Passenger and baggage weight assumptions:
  Passenger weight of 193.6 lb. (88 kg)
  Baggage weight per passenger 37.4 lb. (17 kg) and volume of at least 4 cubic feet per passenger
- (M) 250 nmi Short Takeoff and Landing (STOL) runway mission with 20 passengers
- Maximum takeoff and landing field lengths of 1,500’ over a 50’ obstacle to a runway with dry pavement (sea level ISA + 18°F day).
- Takeoff, and landing performance should also be shown at 5,000’ above mean sea level (ISA + 18°F) as well as for dirt, grass, metal mat, gravel, asphalt & concrete fields at sea level (ISA+18°F).
- (M) 250 nmi Short Takeoff and Landing (STOL) water mission with 20 passengers
- Maximum takeoff distance of 1,900 (sea level ISA + 18°F day) over a 50’ obstacle.
- Takeoff, and landing performance should also be shown at ISA + 18°F at 5,000’ MSL (ISA+18°F).
- (M) Ability to takeoff and land in Sea State 3 conditions
- (T) Ability to takeoff and land in Sea State 4 conditions
- (M) 1000 nmi design range for maximum density passenger mission
- Show takeoff and landing field lengths over a 50’ obstacle to a runway with dry pavement (sea level ISA + 18°F day).
- Show takeoff and landing field lengths from water (sea level ISA + 18°F day).

1.2.3 Cargo Mission:

- (M) 5,000 lb. payload
- (M) 500 nmi range
- Show takeoff and landing field lengths over a 50’ obstacle to a runway with dry pavement (sea level ISA + 18°F day).
- Show takeoff and landing field lengths from water (sea level ISA + 18°F day).
- (M) Ability to unload, refuel and load cargo in no more than 60 minutes
- (T) Ability to carry odd shaped cargo or a standard container

1.2.4 Surveillance Mission:

- (M) 3,000 lb. or greater payload
- (M) 10-hour endurance at 500’ above the water (ISA + 18°F day)
- 2017 Multi-Mission Amphibian (MMA) Undergraduate Team Design Competition

- Show takeoff and landing field lengths over a 50’ obstacle to a runway with dry pavement (sea level ISA + 18°F day).
- Show takeoff and landing field lengths from water (sea level ISA + 18°F day).
- (T) 12 hour or greater endurance

- (M) 150 knot cruise
- (T) 200 knot or greater cruise speed

1.3 Design Method

This report utilizes the design method which is outlined in [1]. The design starts with an initial weight estimate which is a result of considering both competitor aircraft and statistical equations. This allows to design the wings and decide on which engine should be used. This is based on the critical performance parameters such as power to weight ratio and wing loading. After this, geometric properties of the aircraft are clear so that drawing can be done. While drawing the aircraft, Open VSP program is used. When the geometry of the aircraft is decided, then center of gravity and major components of the aircraft can be calculated. Hence, longitudinal stability of the aircraft could be calculated. After that, aerodynamic properties of the aircraft and thrust correction of the engine can be done. Also, most of the components of the aircraft is calculated again by using statistical method. Finally carpet plots are obtained and power and wing loading levels are optimized to meet the requirements with minimal weight.

1.4 Competitor Study

Airplane design is an evolutionary, rather than revolutionary, process. Which means a lot can be learned from studying aircraft of the same category when designing a new aircraft. Some important characteristics of aircraft similar in role, payload and range to the requirements were compiled. For this part, information gathering from the [2], [3], [4], [5], [6], [7].

1.5 Performance Parameters

Table 1 Performance Parameters of the Competitors' Aircrafts. N/F: Not Found

Design Requirements	Canadair CL-215	Dornier Seastar	DHC-6 Twin-Otter	ShinMaywa US-2	Harbin SH-5	Bombardier 415
Crew	2	2	2	11	8	2
Cruise Speed [kts]	157	184	150	260	243	180
Service Ceiling (ft.)	14,700	14,800	26,700	23,606	20,000	14,700
Take-off distance (ft.)	2,755	2,250	1,500	1610	1804	2,750
Range (nm.)	1,131	1,000	775	2,540	2,570	1,320
Payload (lb.)	-	4,000	4,250	-	13,000	6,400
Number of Passengers	26	12	20	20	N/F	N/F

1.5.1 Geometric Characteristics

Table 2 Geometric Characteristics of the Competitors' Aircrafts

Geometric Characteristics	Canadair CL-215	Dornier Seastar	DHC-6 Twin-Otter	ShinMaywa US-2	Harbin SH-5	Bombardier 415
Length (ft.)						
Wing Span (ft.)	93.84	50.9	65	108.75	108.08	93.95
Wing Area	1,080	329	420	1,462	1,550	1,080
Aspect Ratio	8.15	8.45	10.00	8.00	9.00	8.20
Height (ft.)	29.25	15.9	19.5	32.16	32.08	29.25
Empty Weight (lb.)	26808	5290	6880	56500	55100	28400
Design TO (lb.)	37700	9260	12500	105160	99200	43850

1.5.2 Design Characteristics

Table 3 Design Characteristics of the Competitors' Aircrafts

Design Characteristics	Canadair CL-215	Dornier Seastar	DHC-6 Twin-Otter	ShinMaywa US-2	Harbin SH-5	Bombardier 415
W/S	34.91	30.20	29.76	71.93	64.00	40.60
P/W	0.11	0.11	0.11	0.17	0.13	0.11
Stall Speed (kts.)	66	62.55	58	N/F	92	68
W_e/W_0	0.711	0.571	0.550	0.537	0.555	0.647
W_f/W_0	0.277	0.330	0.201	N/F	0.367	0.234

2 Chapter 2 – Initial Sizing

2.1 Weight of the Mi-1 and Its First Estimation

2.1.1 Simple Cruise Mission Sketch

In this part, mission segments are observed. From the requirements, there is three different mission profile. They have similar mission segments. This mission segments shown in the below mission sketch.

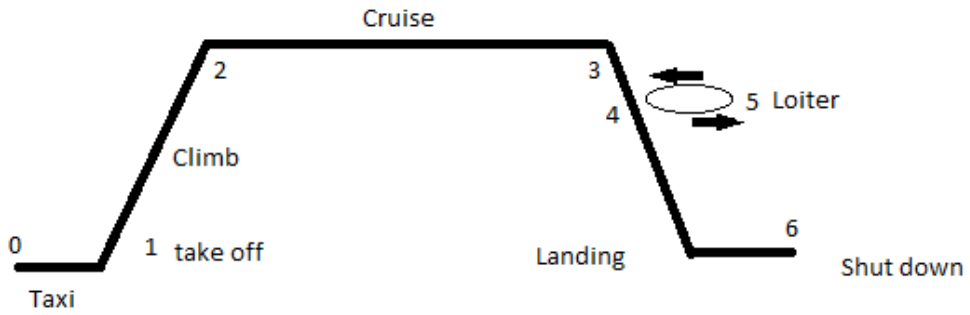

Figure 1 Simple cruise mission profile sketch

Design gross weight, W_0, is made up of four parts; crew weight, W_c, payload weight, W_p, fuel weight, W_f and empty weight, W_e.

$$W_o = W_{crew} + W_{payload} + W_{fuel} + W_{empty} \rightarrow W_o = \frac{W_{crew} + W_{payload}}{1 - W_{fuel}/W_o - W_{emty}/W_o}$$

Empty weight fraction for a cargo bombers' statistical value is used from the table 3.1 of [1] for flying boat:

$$\frac{W_{emty}}{W_o} = 1.09 * W_0^{-0.05}$$

Fuel consumption will be calculated as mission segment fuel weight fractions and then multiplied together to receive overall fuel spending.

$$\frac{W_6}{W_0} = \frac{W_6}{W_5}\frac{W_5}{W_4}\frac{W_4}{W_3}\frac{W_3}{W_2}\frac{W_2}{W_1}\frac{W_1}{W_0}$$

Mission segment fuel weight fraction from instant 0 to instant 1 and from instant 1 to 2 will be assumed to be 0.97 and 0.985 respectively based on historical trends. For calculating mission segment fuel weight fraction from instant 2 to 3, Breguet range equation was used turboprop engines.

$$\frac{W_3}{W_2} = e^{-\frac{RC_{cruise}}{550 * n_p * \left(\frac{L}{D}\right)_{max}}}$$

Note that L\D ratio is estimated from the fig 3.6 of [1] which is based on the value of the $S_{ref}\backslash S_{wet}$ ratios for flying boat and relations with Aspect ratio with help of competitor aircraft which is from the fig.3.5 of [1]. Specific fuel consumptions are found from the turboprop engines. Mission segment fuel weight fraction for descent from instant 4 to 5 could be chosen as 1. Mission segment fuel weight fraction for loiter from instant 4 to 5 can be calculated from endurance version:

$$\frac{W_5}{W_4} = e^{-\frac{EC_{loiter}}{\left(\frac{L}{D}\right)_{loiter}}} = 0.9863$$

Endurance is a loiter time that chosen as 20 min or 1200 sec. Loiter L\D value can be found from the following correlation of the [1] for the aircraft with propellers:

$$\left(\frac{L}{D}\right)_{loiter} = 0.866\left(\frac{L}{D}\right)_{max}$$

Mission segment fuel weight fraction for landing from 5 to 6 could be chosen as 0.995 from historical trends which is from [1]. For trapped fuel correction below equation is used:

$$\frac{W_f}{W_0} = 1.06\left(1 - \frac{W_6}{W_0}\right) = 0.1440$$

Final design weight's generalized form can be shown in below. Other mission's payload and passenger' weight and fuel weight fraction should be different.

$$W_o = \frac{5250.9lb}{1 - 0.1440 - 1.09W_0^{-0.05}}$$

2.1.2 TRADE STUDIES

2.1.2.1 Range Trade

The figure below shows how design gross weight of the aircraft changes with changing range.

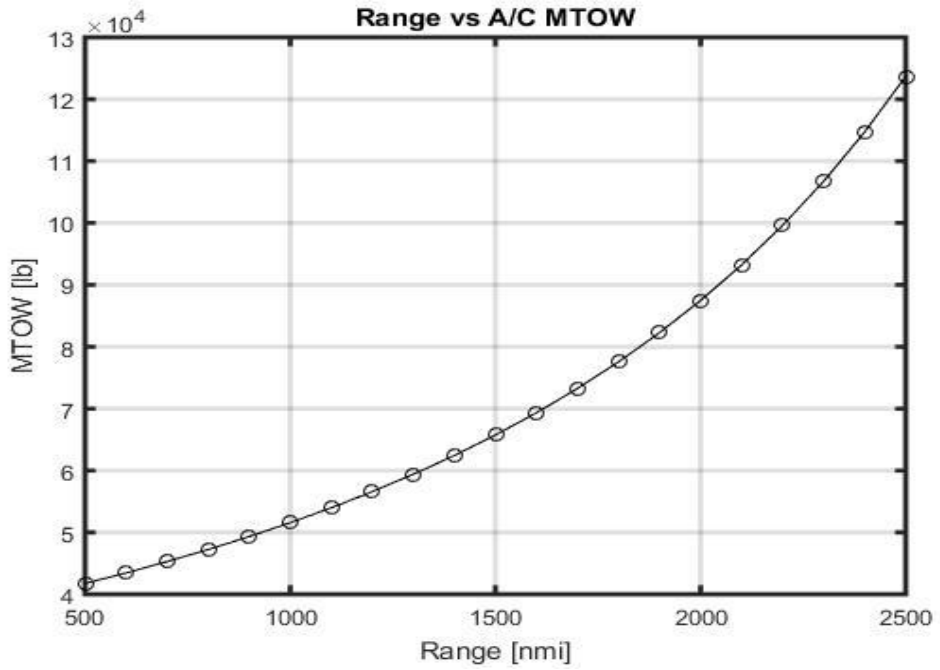

Figure 2 Normal A/C's MTOW (lb) vs Range (nmi)

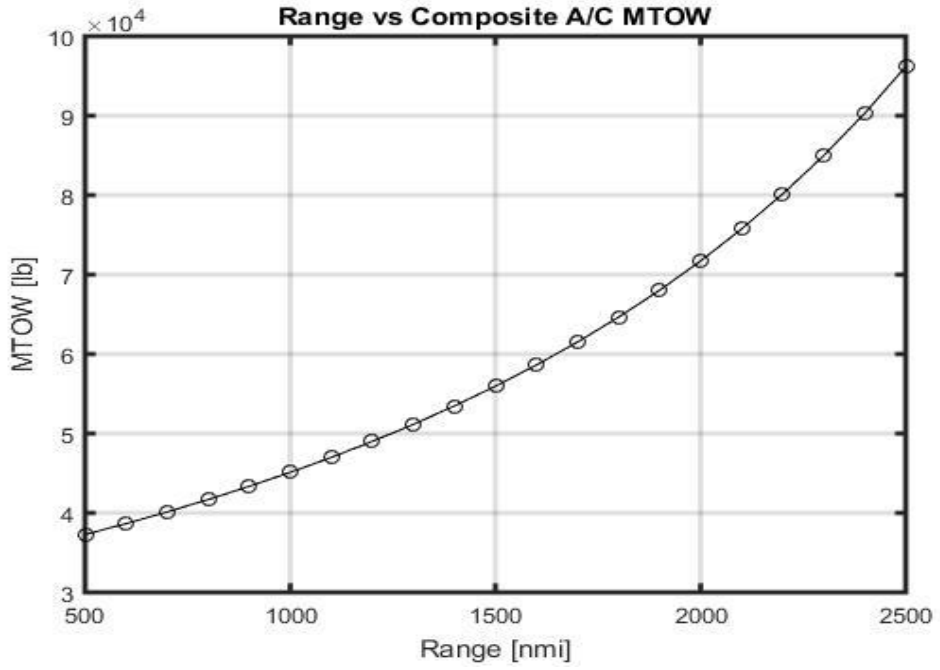

Figure 3 Composite A/C 's MTOW (lb) vs Range (mni). MTOW: Maximum Takeoff Weight

2.1.2.2 Cruise Speed Trade

The figure below shows how design gross weight of the aircraft changes with changing cruise speed.

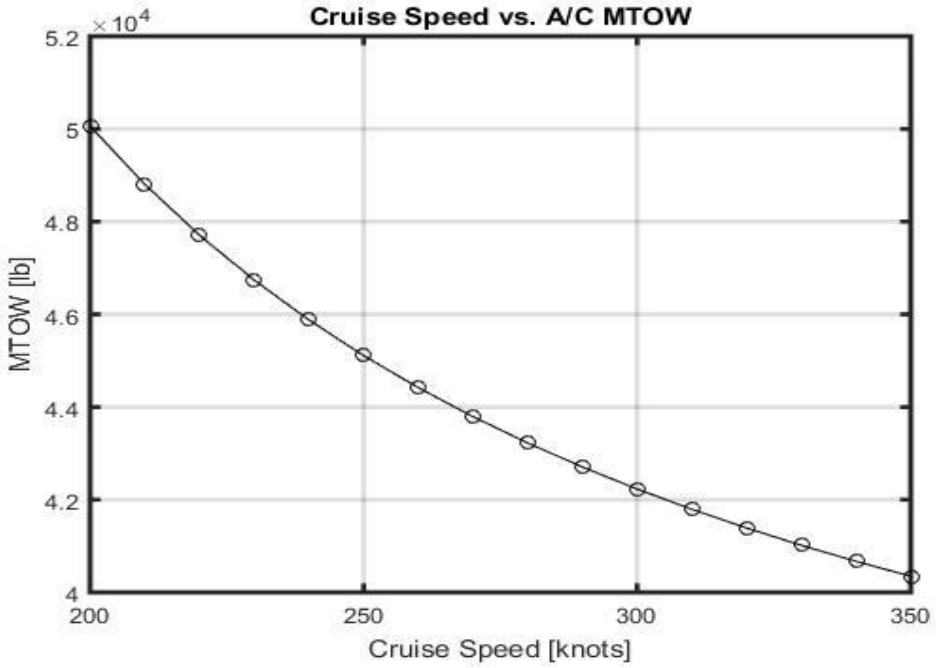

Figure 4 MTOW (lb) vs Cruise Speed (kts)

2.1.2.3 Composite Material Trade

According to [1], empty weight of the aircraft could be decrease as much as %5. Therefore, m constant used as composite material multiplier so that new design weight calculated as below equation. m changes with from 0.95 to 1 with 0.01 increment.

$$W_o = \frac{W_{crew} + W_{payload}}{1 - W_{fuel}/W_o - (W_{emty}/W_o)m}$$

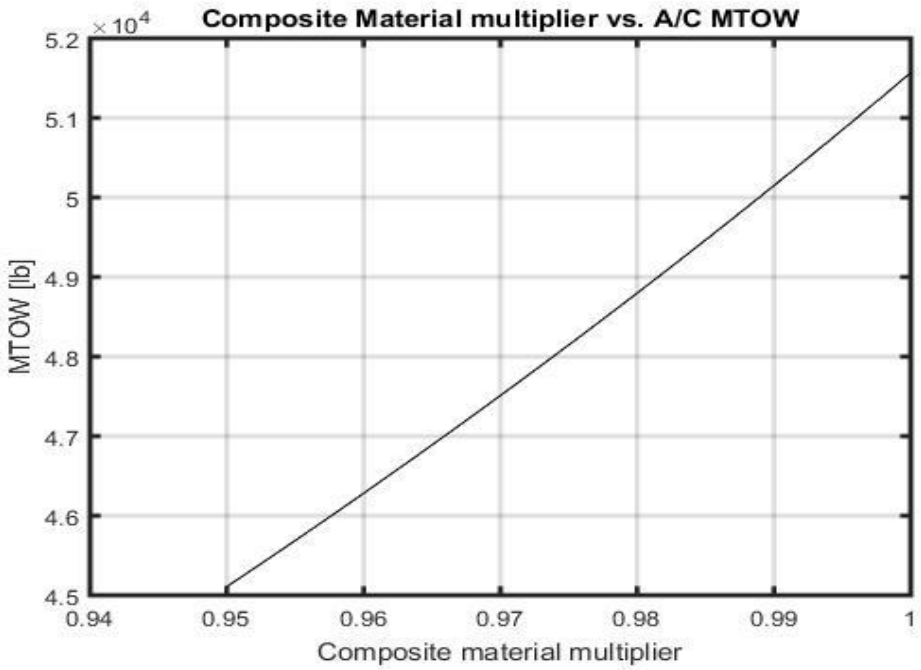

Figure 5 MTOW vs Composite Material Multiplier

From the results one can easily see that aircraft without composite have a highest design weight. This difference could be 30,000 [lb] at highest range. There is a negative correlation between the cruise speed and the design weight. For optimum speed and optimum range, design weight changes between 40,000-60,000 [lb]. In the following parts, this knowledge will be used as a guideline.

2.2 Airfoil and Geometry Selection

2.2.1 Airfoil Selection

There are two main parameters used in airfoil selection. These are design lift coefficient, that is, the coefficient of lift used in most of the aircraft's flight time, and thickness ratio. Design lift coefficient is calculated based on cruise conditions using lift equation. We make use of the assumption that W=L during cruise.

$$W = L = 0.5 * \rho_\infty * S * c_L * V_\infty^2 \rightarrow c_L = \frac{W}{S} * \frac{2}{\rho_\infty * V_\infty^2}$$

Density of the air from [8] chosen from 25000 ft. which is think as service ceiling altitude. Moreover, cruise speed is chosen as 250 knots. Wing loading calculated from the average of competitors' wing loading. Hence, we find design lift coefficient $c_L = 0.4774$.

For finding a suitable airfoil, one needs environment conditions. For that case Reynolds Number is used. Reynolds number should be minimum for stall conditions of the aircraft at sea level. Reynolds Number is found by below equations. Numbers are used in form of imperial units.

$$Re = \frac{V_{stall} * \bar{c} * \rho_{\infty}}{\mu_{\infty}} = \frac{(113) * (10.15) * (23.77 * 10^{-4})}{(3.737 * 10^{-7})} \rightarrow Re = 7{,}295{,}424$$

Our aircraft speed changes between 0.3 M and 0.4 M. Therefore, historical trend from the fig 4.14 of [1] indicates a thickness ratio between 14-16% to choose. This information is then used to check competitor airfoils to the following result:

Table 4 $C_{l,max}$ and $C_{m,0}$ values of the airfoils

	$C_{l,max}$	$C_{m,0}$ **(absolute value)**
Canadair CL-415: NACA 4417	2,02 at 18 degrees	0,09
Dornier Seastar: NACA 23015	1,625 at 16 degrees	0,0045
DHC-6 Twin Otter: NACA 63A516 Modified	1.656 at 12 degrees	0.1

Among these airfoils NACA 4417 offers very good moment characteristics and the highest maximum coefficient of lift. The stall angle of attack is also higher for this airfoil. Thus NACA 4417 was chosen for this aircraft.

2.2.2 Wing Sweep and Taper Ratio

Taper ratio affects the induced drag, structural weight of the airfoil and the tip stall characteristics. A taper ratio of around 0.5 is good for reducing the induced drag. For a reduced wing structural weight, taper ratio must be decreased as much as possible. However, tip stall characteristics become a problem if the taper ratio is too low. Considering these effects, a taper ratio of 0.5 is selected.

Leading edge sweep of the comparable aircraft are zero or near zero. However, in this aircraft, a taper ratio that is smaller than 1 is used. This means that either leading edge sweep or trailing edge sweep or both are not going to be zero. It was decided that the leading-edge sweep and the trailing edge sweep are to be equal.

A high wing configuration must be used to keep the engine, propellers and the wing away from the water. To increase the stall characteristics and reduce the wing rocking, a common value of 2 degree is selected for the twist.

2.3 Power to Weight and Wing Loading

Power to weight ratio and wing loading are perhaps two of the most important performance parameters of an aircraft. These two parameters determine how the aircraft will perform in virtually all performance related maneuvers and flight conditions.

Power to weight ratio P/W_0 is usually defined as the ratio of power of all the engines at maximum throttle settings at sea-level static and standard-day conditions divided by the design takeoff weight of the aircraft. Power to weight ratio P/W_0 has a direct effect on the performance of an aircraft. A higher Power to weight ratio will result in higher acceleration, quicker climb, higher maximum speeds and higher turn rates. However, Power to weight ratio requires for more powerful and thus larger engines. Power to weight ratio of historical trend from the table 5.2 of [1] is 0.1 hp/lb . Additional, average of the competitors' power to weight ratio is found 0.123 hp/lb .

2.3.1 Wing Loading

Wing loading shows how much weight, each of the wing reference area carries at a given flight condition. A smaller wing loading results in a larger wing. Wing loading will be calculated for each performance requirement and the largest wing loading that satisfies all the requirements will be selected at the end. This makes sure that the smallest possible wing is designed.

2.3.1.1 Cruise Wing Loading

The main objective in cruise is to increase range. This is done by increasing aerodynamic efficiency of the aircraft, or in other words, maximizing L/D in propeller airplanes. This happens when induced drag is equal to parasite drag.

$$\frac{W}{S} = q_\infty * \sqrt{\pi * AR * e * C_{D0}}$$

Dynamic pressure term can be calculated from cruise condition parameters of density and speed. Aspect ratio term come from the competitors' average value. Oswald span efficiency factor can be calculated from this equation:

$$e = 1.78 * (1 - 0.045 * AR^{0.68}) - 0.64 \rightarrow e = 0.7926$$

Also, parasite drag coefficient can be approximately calculated as $C_{D0} = 0.02$.

2.3.1.2 Loiter and Endurance Wing Loading

Wing loading from the loiter can be found from the similar equation. Endurance is maximized when the induced drag is three times of the parasite drag which shown as:

$$\frac{W}{S} = q_\infty * \sqrt{3 * \pi * AR * e * C_{D0}}$$

2.3.1.3 Wing Loading from Takeoff Distance

The ‘’obstacle clearance distance’’ is the distance required from brake release until the aircraft has reached until the aircraft has reached some specified altitude. For this design, it is 50 ft. Both the wing loading and the power to weight ratio contribute to the takeoff distance. Fig. 5.4 of the [1] provides graphs for approximating the “Takeoff parameter” defined as:

$$TOP = \frac{W/S}{\sigma * C_{L,TO} * P/W} \rightarrow \frac{W}{S} = TOP * \sigma * C_{L,TO} * P/W$$

Here σ is the ratio of air density at takeoff location divided by air density at sea level. For the purposes of this, it will be assumed that the aircraft takes off from sea level making the value of σ equal to 1. Power to weight ratio is assumed as average of the competitors. From the reference [1] ,

$C_{L,TO} = \frac{C_{L,max}}{1.21}$. Again, from the fig. 5.3 of [1], $C_{L,max}$ is estimated as 2.5. Therefore, $C_{L,TO}$ is calculated as 2.

2.3.1.4 Landing Distance

Reference [1] provides an equation for estimating the wing loading based on landing distance.

$$S_{landing} = 0.66 * 80 * \left(\frac{W}{S}\right) * \left(\frac{1}{\sigma * C_{L,max}}\right) + S_a$$

S_a is obstacle clearance distance and assumed as 750 ft. The term which is 0.66 implies that our aircraft is equipped with reversible-pitch propellers. For the passenger mission, required landing distance is 1500 ft.

2.3.2 Power-to Weight Ratio

To find the power to weight ratio, P=TV equation is used so that maximum power can be calculated. Since change in the altitude change the power output of the engine, maximum power estimated as 1.67 times of the power which is needed in the service ceiling altitude. Propulsive efficiency of the engine assumed as 0.9. Two different power is calculated in the one mission. One of them is cruise and the other one is the endurance segment. Cruise speed is taken as 250 knots and endurance speed taken as the 200 knots. Since they have different aerodynamic characteristics and speed, their thrust values will be different. Therefore, their power out will be different. Among the two values, highest one is chosen. Previous calculations for the wing loading is used for the finding power to weight ratio.

Table 5 Wing Loading and Power to Weight Ratio Results

	Landing	Take-off	Cruise	Loiter& Endurance
W0/S	41.7781	52.7732	65.5634	95.5186
P/W	0.1637			

Among the wing loading values, lowest one is chosen so that it will be more conservative approach for the design. Power to weight ratio of the Mi-1 is high compared to competitors except the ShinMaywa US-2. However, it is in the acceptable limits.

3 Chapter 3 – Refined Sizing

3.1 Geometry Sizing and Configuration

3.1.1 Fuel Volume

For the fuel the type Jet-A is choosing. Because it is also used in the CL-415. Which is average density is taken as the 6.7 $lb/gallons$. Gallon type is used for US. From the earlier calculations fuel weight taken as 7000lb. From these value, fuel volume can be found as:

$$V_{fuel} = \frac{7000}{6.7}(gal\ to\ ft^3) = \ \ 169.9035 ft^3$$

Our mandatory cruise speed is 200 knots and tradable cruise speed is 250 knots from the requirements of the AIAA competitions. We choose our cruise speed for these calculations as 250 knots. Internal type fuel integration systems are used for wing. 100 percent of fuel carried by wings. Since fuel volume increases at hot days in summer, %5 percent fuel expansion is considered.

$$V_{fuel_{wings}} = V_{fuel} * 1.05 = \ \ 168.8319 ft^3$$

3.1.2 Fuselage Length

Using the equations from the table 6.3 of the [1] result in a fuselage length of 80.83 ft. for this aircraft. Average fuselage length of the competitors was previously found to be 76.6 ft.

3.1.3 Wing Sizing and Planform Shape

Wing area is calculated from weight and wing loading as S = W0/(W0/S) = 1149.7 ft^2. Then, the below table shows that geometric characteristics are calculated from the equations of [1]. Aspect ratio and taper ratio are used in these equations.

Table 6 Wing Geometric Characteristics

	Wing Span-b	**Root Chord-c_r**	**Tip Chord-c_t**	**MAC-$\bar{c}$**	**Span wise location of MAC-$\bar{y}$**	**Taper Ratio-λ**
Units	$[ft]$	$[ft]$	$[ft]$	$[ft]$	$[ft]$	-
Values	92.85	16.5081	8.254	12.8396	20.6351	0.5

MAC: Mean Aerodynamic Center

3.1.4 Tail Sizing and Planform Shape

When choosing the configuration of the tail the dominant points of influence were the expected heavy wake flow from the wing and the wake from the horizontal tail. Since it is proportional to the size of the wing the rudder would be in jeopardy with such a design. For these reasons, a conventional tail has been decided.

The tails were sized with methods outlined in reference [1]. Vertical tail was placed slightly ahead of horizontal tail to avoid horizontal tail wake on the vertical tail in high angles of attack. The following table summarizes tail properties.

Table 7 Horizontal and Vertical Tail Geometric Characteristics

Tail	Area-S	AR	Taper Ratio	Moment Arm	Span-	Root Chord, c_r	Tip Chord, c_t	*MAC*, $\bar{c}$	$\bar{y}$
Unit	$[ft^2]$			$[ft]$	$[ft]$	$[ft]$	$[ft]$	$[ft]$	$[ft]$
Horizontal	232.42	4	0.5	44.46	30.49	10.16	5.08	4.91	6.77
Vertical	158.48	1.2	13.79	40.42	13.79	17.03	5.96	12.38	2.89

3.1.5 Engine and Propeller Dimension and Weight

Power to weight ratio requirement of the aircraft is 0.1637. Using the assumption that MTOW is 52,000 lb, aircraft need 8512 shp (shaft horse power). Since it has two engines, one engine should have 4256 shp . Using conservative approach, we picked the PW150A engine with 5000shp (Alternative option is the Rolls Royce AE 2100J with 4500shp). Engine and propeller properties are given below according to [9]:

Table 8 Engine and Propeller Properties

Engine	Weight	Height	Width	RPS	Propeller	Diameter	Weight
Units	$[lb]$	$[ft]$	$[ft]$	$[1/s]$	**-**	$[ft]$	$[lb]$
PW150A	1060	3.67	2.5	17	**Dowty R414**	13.5	870

RPS: Revolution Per Second

3.2 Hull Design

Hull design is made by using equations from [3]. Hull shape should be designed by starting from load at water rest. Then static beam loading coefficient is calculated and the dimensions of forebody, afterbody. Load at water rest is found as 52000. Beam length is 8.75 ft. Density of the water assumed as 64 lb/ft^3. Therefore, static beam loading coefficient (C_{Δ_0}) is found from the [3]:

$$C_{\Delta_0} = \frac{52000}{(64)(8.75^3)} = 1.21$$

For hull design, forebody length also should be considered. For this length, spray coefficient (K) is used according to [3]. Satisfactory spray coefficient is 0.0675. Hence forebody length is:

$$l_F = b\sqrt{\frac{C_{\Delta_0}}{K}} = 8.75\sqrt{\frac{1.21}{0.0675}} \quad \rightarrow \quad l_F = 37.05ft$$

Keel length is $l_c = 1.7\ b = 14.875$ from step to nose. Bow height is selected from [3] as $h_b = 0.8b$ which has reasoning for good spray conditions on calm and rough water. Afterbody length is found from Looke's approach which in the [3]:

$$l_a = 2.5C_{\Delta_0}^{1/3}b = 2.5\ (1.21)^{1/3}\ 8.75 = 23.3ft$$

Deadrise angle of the forebody is 22 degrees between step and the bow (after half) and slightly increases from bow start up to nose (front half). This approach gives us low hump resistance by after half and good spray by front half according to the Tomaszewski from [3]. It also enhances the cleanness of going through waves. Afterbody Deadrise angle is 30 degrees. Slight bigger Deadrise angle than forebody, increases the ventilation, upgrades porpoising stability in planning region (whole hull) and reduces effect of skipping. Sternpost angle is chosen as 7 degrees from the Gudmunsson from [4] for enough angle of attack for the take-off from water at first. However, it is not satisfactory while calculating buoyancy so it reduced to the 6.86 degrees. Note that, ShinMayva US2 has 5 degrees and CL 415 has 6 degrees of sternpost angles.

3.3 Preliminary CG Estimation

3.3.1 Weight Estimation of Main Components

It is decided that the keep fuel tanks in the wing. Two wing tanks have 99 [ft^3] volume for each of them to be conservative. Cross section of tanks is not fixed. They can be easily upgraded to have much volume. Fuselage length is found from the previous calculations. L_f=80.83 [ft]. For the wing, NACA 4417 Airfoil is used.

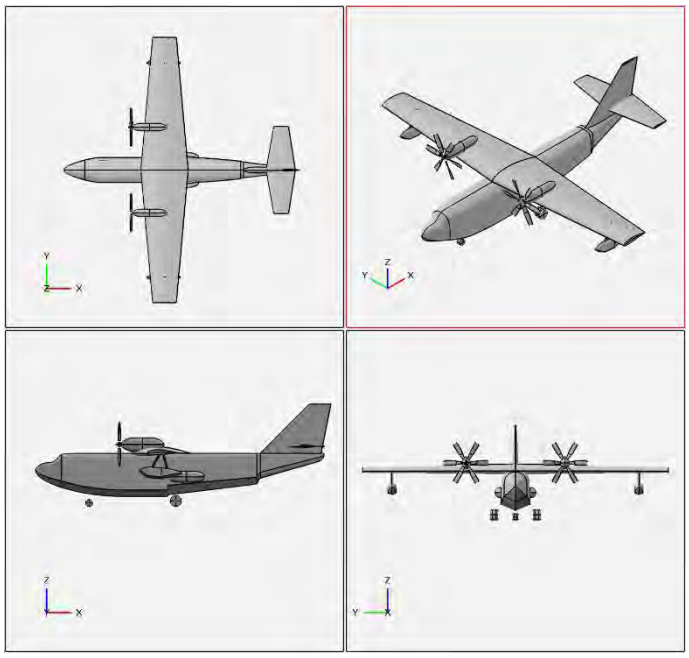

Figure 6 - 4 View of Mi-1

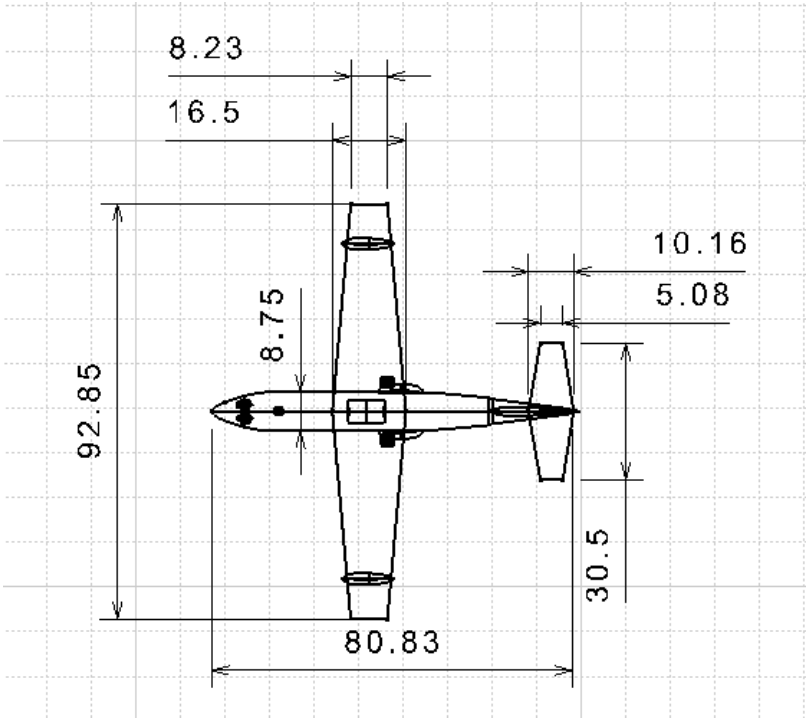

Figure 7 Top view and Dimensions of Mi-1

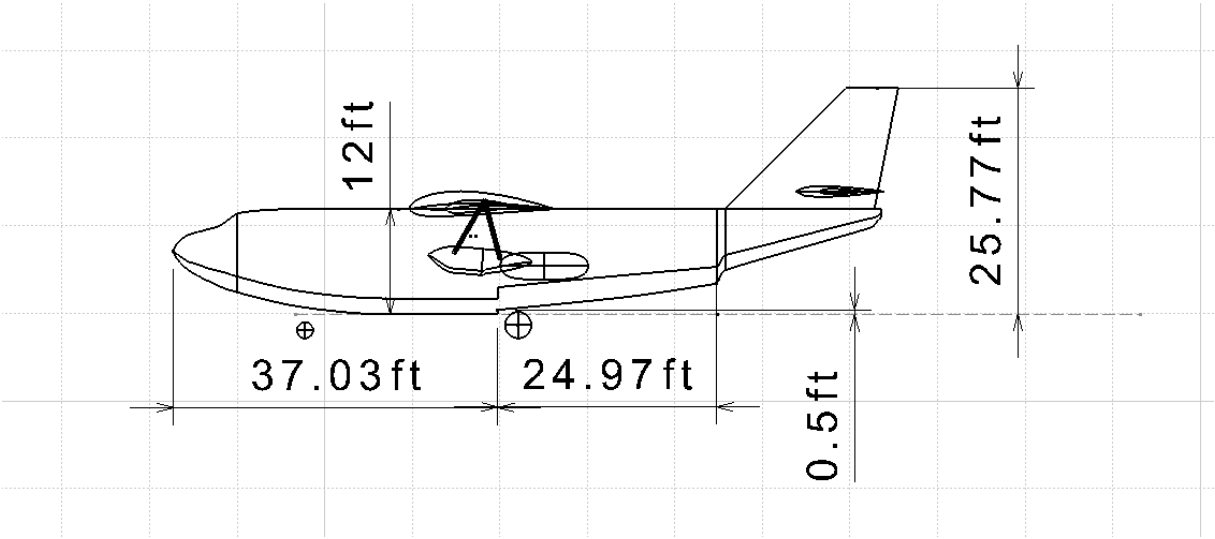

Figure 8 Left View of Mi-1 and dimensions

From reference [1] using closest match, bombers and transport aircraft approximation to calculate empty weight. From Open VSP, these values are found. For all of calculations wetted area is used for approximation. The relation of exposed wing area and the wetted wing area is found from the [4] which gives following correlation by considering the thickness of the airfoil.

$$S_{wet_{wing}} = S_{exposed_{wing}} 2\left(1 + 0.2\left(\frac{t}{c}\right)_{wing}\right)$$

Following correlations are taken from reference [1] for bombers and transport airplanes which we assumed as closest approach to our design. Wing weight is modified to find more plausible results. After the several calculations, weights of the major components of the aircraft found in the given table:

Table 9 Weight of the Major Components of the Aircraft

W_{wing}	W_{HT}	W_{VT}	$W_{fuselage}$	$W_{engine,wet}$	$W_{propeller}$
5572 $[lb]$	1218 $[lb]$	906 $[lb]$	13323 $[lb]$	2756 $[lb]$	1740 $[lb]$

Moreover, calculation of the weights of the landing gear and other parts depends on iterative process from the [1]. Therefore, $W_{landing\ gear} = 1394\ [lb]$ and $W_{All\ else} = 5511\ [lb]$. Finally, empty weight of the aircraft found as $W_e = 32422\ [lb]$. To find takeoff design weight, fuel and passenger weights should be considered. Passenger weight is calculated for 39 passengers and 3 crew members. Also, with their luggage it becomes $W_{passenger} = 9030\ [lb]$. Fuel weight is found as $W_{fuel} = 7000\ [lb]$. Hence, takeoff weight becomes:

$$W_0 = 49144\ [lb]$$

3.3.2 CG calculation and Landing Gear Position

All component CG locations are calculated separately for each component from Open VSP by using "massprop" command. Aircraft CG is found at after putting all components and their weights into excel.

	Weight	X	Y	Z	MX	MY	MZ
Fuselage	13323.275	34.227	0	0	4.56E+05	0.00E+00	0.00E+00
Wing	5572.171	34.151	0	6.435	1.90E+05	0.00E+00	3.59E+04
VT	906.259	73.33	0	10.841	6.65E+04	0.00E+00	9.82E+03
HT	1218.085	75.468	0	8	9.19E+04	0.00E+00	9.74E+03
Fuel	7000.000	34.1	0	6.6692	2.39E+05	0.00E+00	4.67E+04
All Else	5511.670	24	0	0.477	1.32E+05	0.00E+00	2.63E+03
Engine	2756.000	28.5	0	8.5	7.85E+04	0.00E+00	2.34E+04
Prop	1110.000	23.5	0	8.5	2.61E+04	0.00E+00	9.44E+03
Passenger&cargo	9722.286	31.939	0.469	0.463	3.11E+05	4.56E+03	4.50E+03
Land Gear	1394.128	0	0	0	0.00E+00	0.00E+00	0.00E+00
F	209.119	18.427	0	-3.132	3.85E+03	0.00E+00	-6.55E+02
R	1185.009	41.6	0	-3.132	4.93E+04	0.00E+00	-3.71E+03
Total	48513.875				1.64E+06	4.56E+03	1.38E+05
Aircraft-CG		33.88668	9.40E-02	2.84E+00			

Ground clearance is not problem for high wing design. All values are for Dowty R408 propeller from Q400 aircraft.

36X11.0R18 → Rear Landing Gear Tire. 22X7.75-9 → Front Landing Gear Tire according to weight of aircraft.

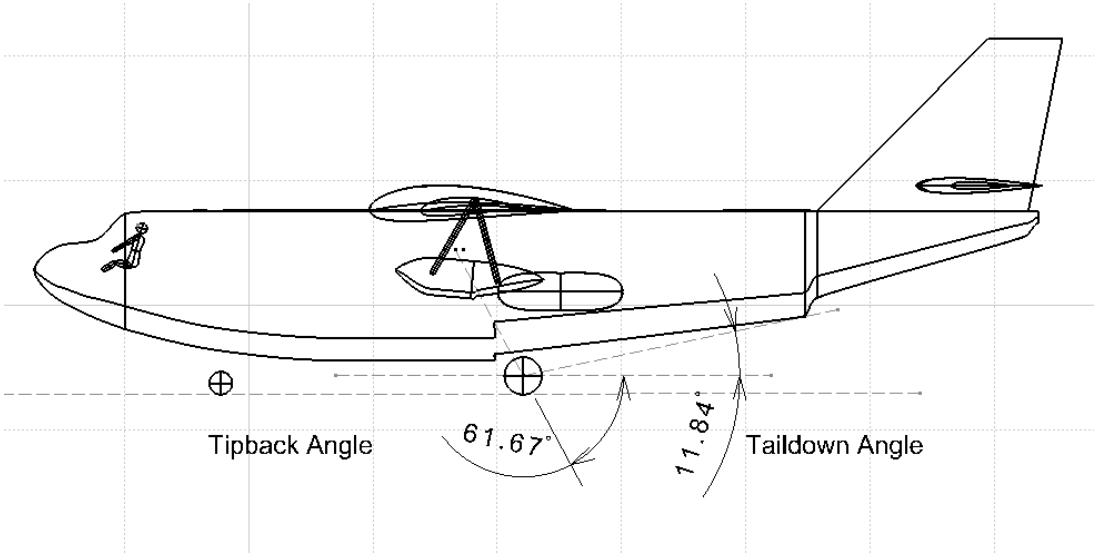

Figure 9 Tipback and Taildown Angles of the Aircrafts

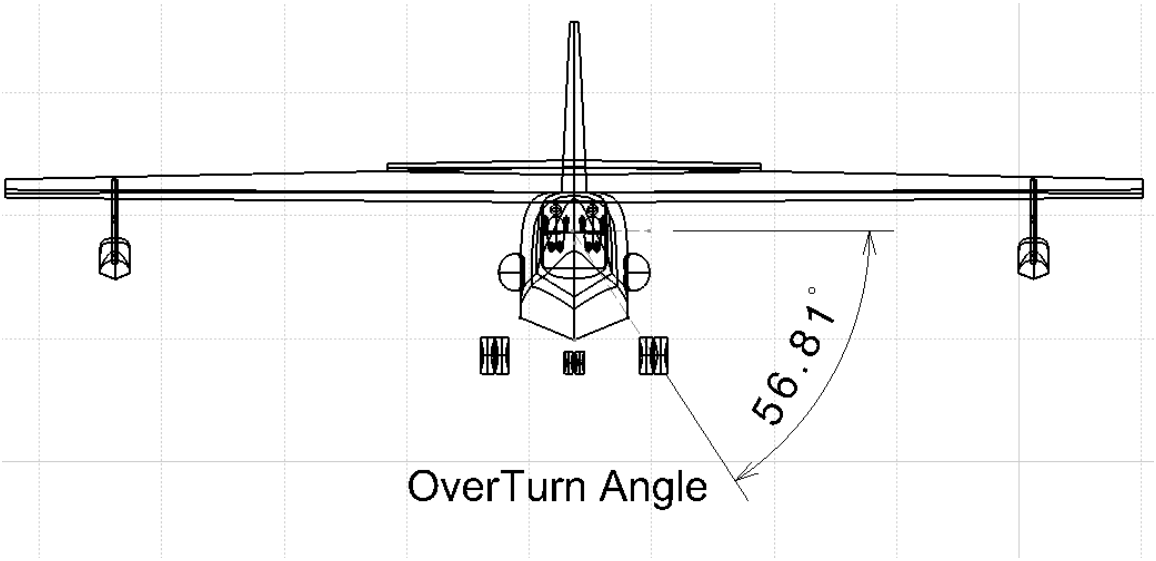

Figure 10 Overturn Angle of the Aircraft

	Angle (degree)		Angle (degree)
Taildown	11.84	**Forebody Flat Deadrise**	22.64
Tipback	28.33	**Forebody Front Deadrise**	30.7
Over Turn	56.96	**Sternpost**	6.86
Afterbody Deadrise	32.13		

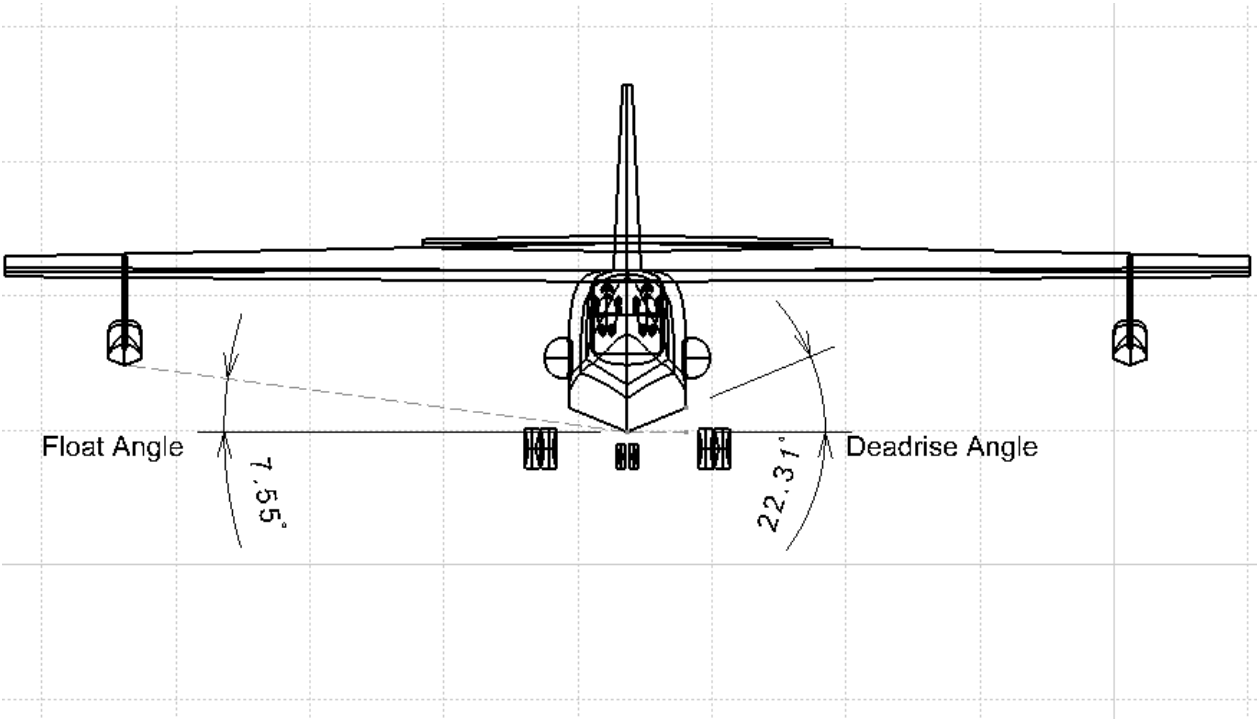

Figure 11 Float angle and Deadrise angle

Float angle from bottom of fuselage is between 7-9 degrees according to [11] and [1]. It corresponds to 7.55 degrees in design. Deadrise angle is 22.31 degrees and

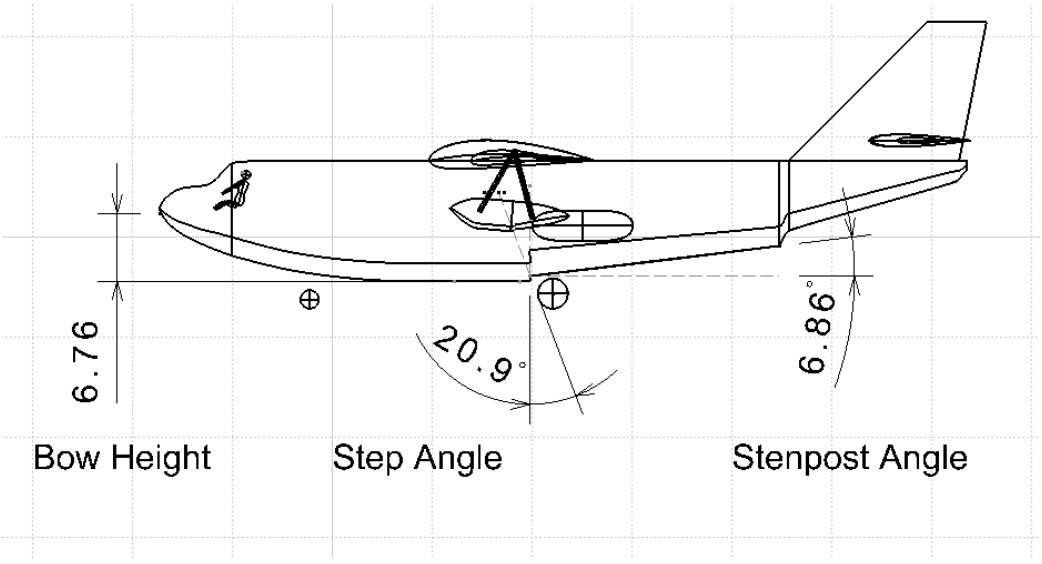

Figure 12 Bow Height and Sternpost Angle of the Aircraft

3.3.2.1 Buoyancy

Buoyancy will be satisfied with 2.5 degrees' rotation with respect to nose in longitudinal plane. Also, it corresponds to 6.86 degrees with respect to CG location and gives incidence angle to the wing. Below case corresponds to 0 distance between CG and buoyancy center in vertical direction.

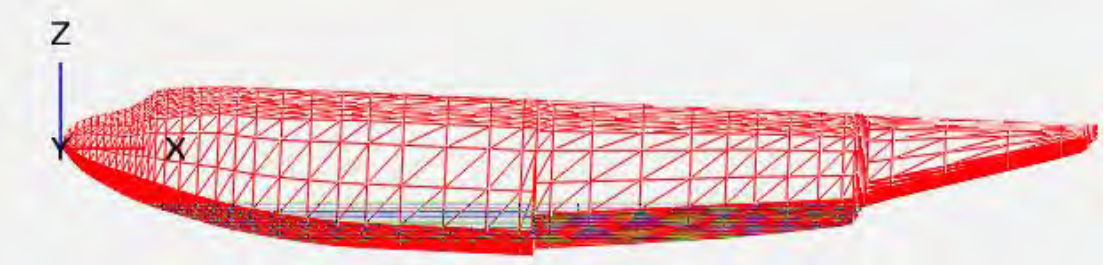

CG location and angle change due to fuel and passengers

3.3.2.2 Half fuel and 39 passengers, no passenger luggage:

	Weight	X	Y	Z	MX	MY	MZ
Fuselage	1.33E+04	34.227	0	0	4.56E+05	0.00E+00	0.00E+00
Wing	5.57E+03	34.151	0	6.435	1.90E+05	0.00E+00	3.59E+04
VT	9.06E+02	73.33	0	10.841	6.65E+04	0.00E+00	9.82E+03
HT	1.22E+03	75.468	0	8	9.19E+04	0.00E+00	9.74E+03
Fuel	3.50E+03	34.1	0	6.6692	1.19E+05	0.00E+00	2.33E+04
All Else	5.51E+03	24	0	0.477	1.32E+05	0.00E+00	2.63E+03
Engine	2756	28.5	0	8.5	7.85E+04	0.00E+00	2.34E+04
Prop	1110	23.5	0	8.5	2.61E+04	0.00E+00	9.44E+03
Passenger&cargo	8.15E+03	28.685	0.469	0.463	2.34E+05	3.82E+03	3.77E+03
Land Gear	1.39E+03	0	0	0	0.00E+00	0.00E+00	0.00E+00
F	2.09E+02	18.427	0	-3.132	3.85E+03	0.00E+00	-6.55E+02
R	1.19E+03	41.6	0	-3.132	4.93E+04	0.00E+00	-3.71E+03
Total	4.34E+04				1.45E+06	3.82E+03	1.14E+05
Aircraft-CG		33.32971	8.80E-02	2.62E+00			

3.3.2.3 Full Fuel and Just Crew:

Note that because of the location of passengers, cg of "passenger and cargo" component moves forward (11ft moves forward ~ assumed according to Open VSP mass command).

	Weight	X	Y	Z	MX	MY	MZ
Fuselage	1.33E+04	34.227	0	0	4.56E+05	0.00E+00	0.00E+00
Wing	5.57E+03	34.151	0	6.435	1.90E+05	0.00E+00	3.59E+04
VT	9.06E+02	73.33	0	10.841	6.65E+04	0.00E+00	9.82E+03
HT	1.22E+03	75.468	0	8	9.19E+04	0.00E+00	9.74E+03
Fuel	7.00E+03	34.1	0	6.6692	2.39E+05	0.00E+00	4.67E+04
All Else	5.51E+03	24	0	0.477	1.32E+05	0.00E+00	2.63E+03
Engine	2756	28.5	0	8.5	7.85E+04	0.00E+00	2.34E+04
Prop	1110	23.5	0	8.5	2.61E+04	0.00E+00	9.44E+03
Passenger&cargo	6.94E+02	21.059	0.469	0.463	1.46E+04	3.26E+02	3.22E+02
Land Gear	1.39E+03	0	0	0	0.00E+00	0.00E+00	0.00E+00
F	2.09E+02	18.427	0	-3.132	3.85E+03	0.00E+00	-6.55E+02
R	1.19E+03	41.6	0	-3.132	4.93E+04	0.00E+00	-3.71E+03
Total	3.95E+04				1.35E+06	3.26E+02	1.34E+05
Aircraft-CG		34.14064	8.25E-03	3.38E+00			

3.3.2.4 Half fuel, full luggage, no passengers:

	Weight	X	Y	Z	MX	MY	MZ
Fuselage	1.33E+04	34.227	0	0	4.56E+05	0.00E+00	0.00E+00
Wing	5.57E+03	34.151	0	6.435	1.90E+05	0.00E+00	3.59E+04
VT	9.06E+02	73.33	0	10.841	6.65E+04	0.00E+00	9.82E+03
HT	1.22E+03	75.468	0	8	9.19E+04	0.00E+00	9.74E+03
Fuel	3.50E+03	34.1	0	6.6692	1.19E+05	0.00E+00	2.33E+04
All Else	5.51E+03	24	0	0.477	1.32E+05	0.00E+00	2.63E+03
Engine	2756	28.5	0	8.5	7.85E+04	0.00E+00	2.34E+04
Prop	1110	23.5	0	8.5	2.61E+04	0.00E+00	9.44E+03
Passenger&cargo	1.57E+03	28.148	0.469	0.463	4.43E+04	7.38E+02	7.29E+02
Land Gear	1.39E+03	0	0	0	0.00E+00	0.00E+00	0.00E+00
F	2.09E+02	18.427	0	-3.132	3.85E+03	0.00E+00	-6.55E+02
R	1.19E+03	41.6	0	-3.132	4.93E+04	0.00E+00	-3.71E+03
Total	3.69E+04				1.26E+06	7.38E+02	1.11E+05
Aircraft-CG		34.13505	2.00E-02	3.00E+00			

According to above CG calculations for different passenger configurations with conservative approach.

CG	X-location [ft]
Standard	33.89
Most forward	33.33→33.0
Most rearward	34.14→34.5

Individual CG locations of fuel tanks and passenger seats are very close to the CG location, so location change is very low.

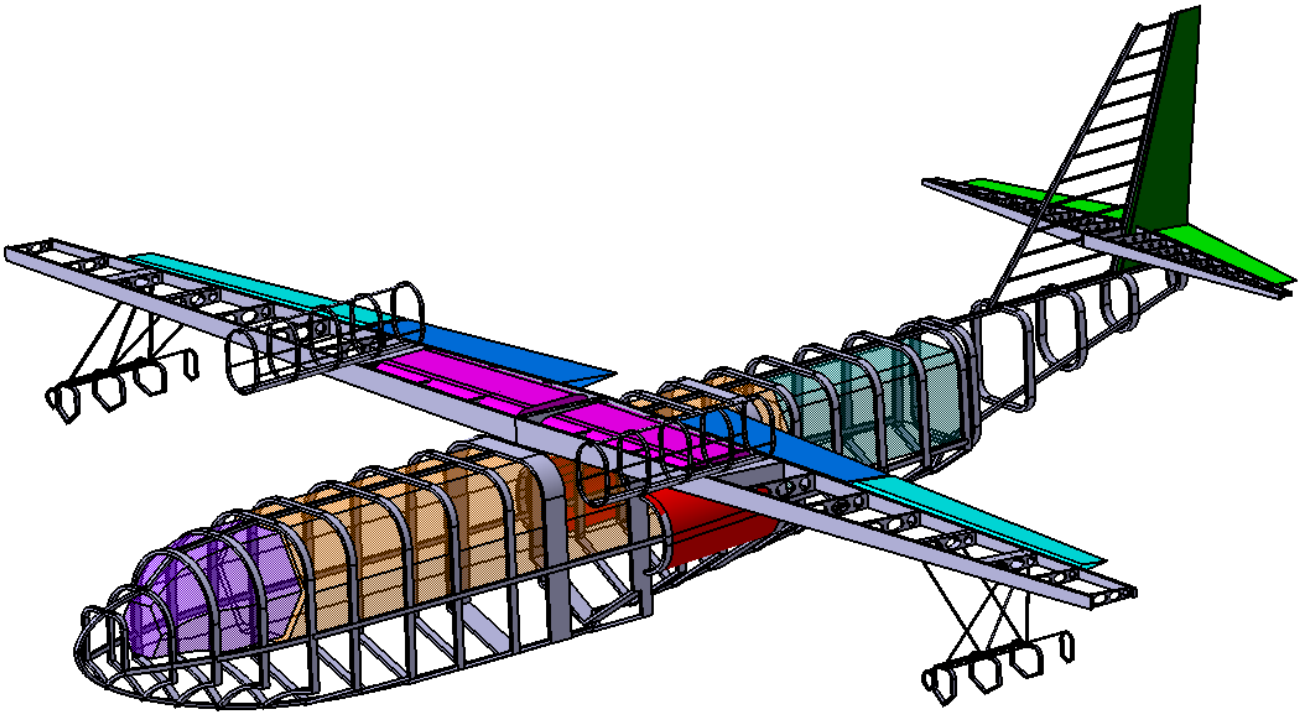

Figure 13 Components of the aircraft

Color	***Component***	***Color***	***Component***
Blue	Flaps	**Green**	Elevator
Cyan	Ailerons	**Dark Green**	Rudder
Red	Landing Gear	**Pink**	Fuel Tanks
Black	Side Float Structure	**Purple**	Flight Deck
Orange	Passenger Compartment	**Turquoise**	Cargo
Gray	Main Structural Elements: Spars, Engine Mount, Hull, Ribs, Struts		

Aircraft structure must be light and durable. An amphibian aircraft must have different kind of design for bottom of the fuselage. Above figure does not show that; however, it must have same configuration with a boat float.

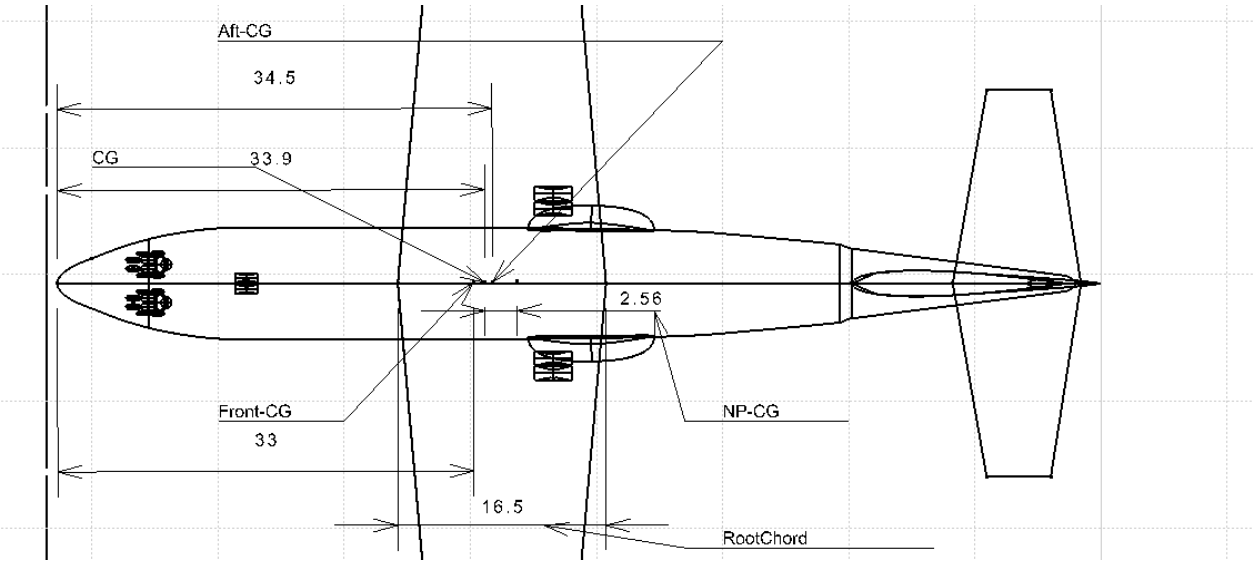

Figure 14 CG locations of the aircraft

3.3.3 Compartment Layout

3.3.3.1 Pilot Sight

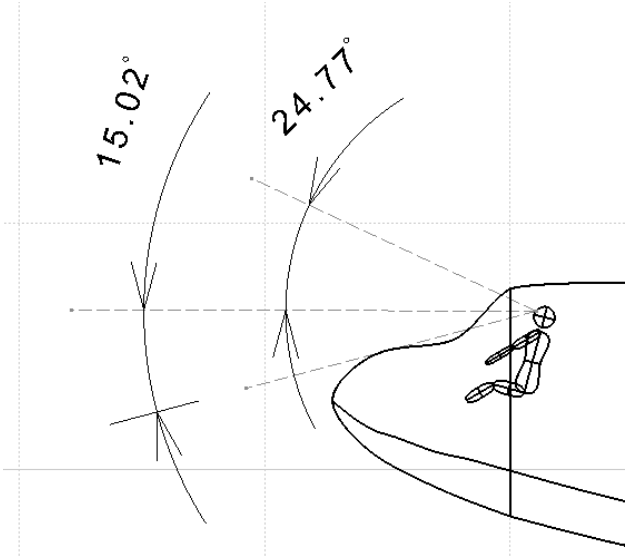

Figure 15 Pilot Front Vision

Pilot sight is 15 degrees to bottom and 24.77 degrees to top.

3.3.3.2 Passenger and Luggage Layout

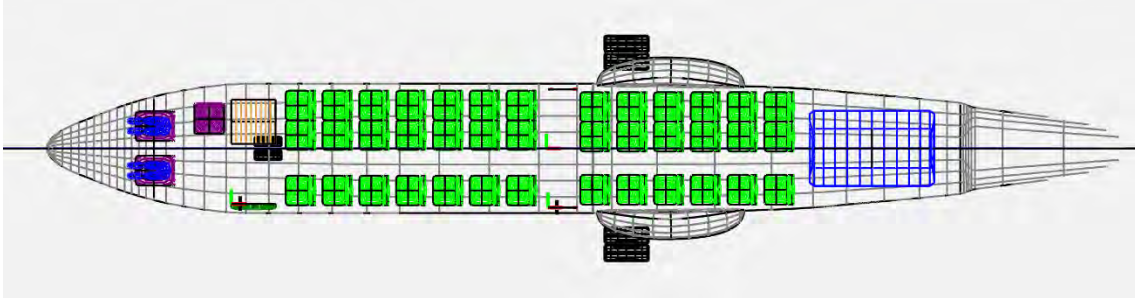

Figure 16 Passenger Layout

Passenger Compartment is as figure above and it has two emergency exits in middle and there is an entry gate in front of the passenger compartment.

3.3.3.3 Surveillance Layout

Surveillance layout is as follows. 7 seats are shown in purple for crew and blue “podman” are for the flight crew. 3000lb payload is at the back.

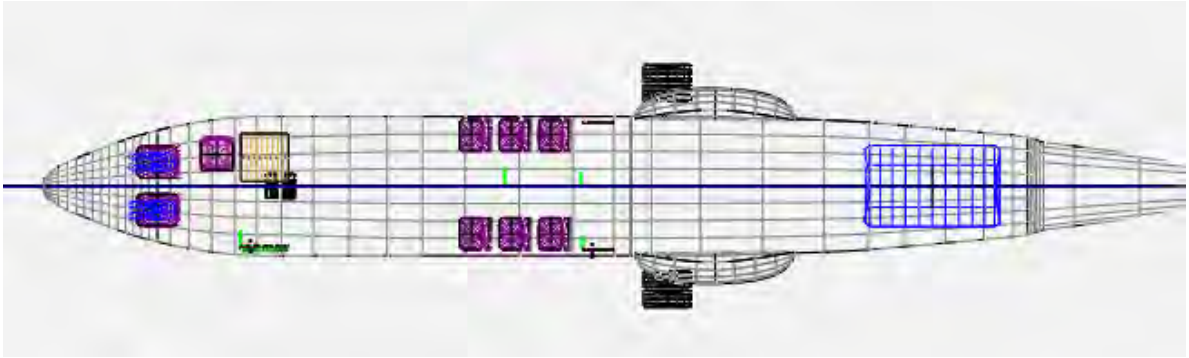

Figure 17 Surveillance Mission Layout

3.3.3.4 Cargo Layout

Cargo compartments are shown below. Blue rectangles are suitable for standard container with 96’’ length, 64’’ height and 60.4’’ cargo which can carry 5399lb. 2 cargo containers can be organized for suitable CG location. Cargo configuration with one container should be put according to CG location. There are two additional seats (purple) for cargo crews.

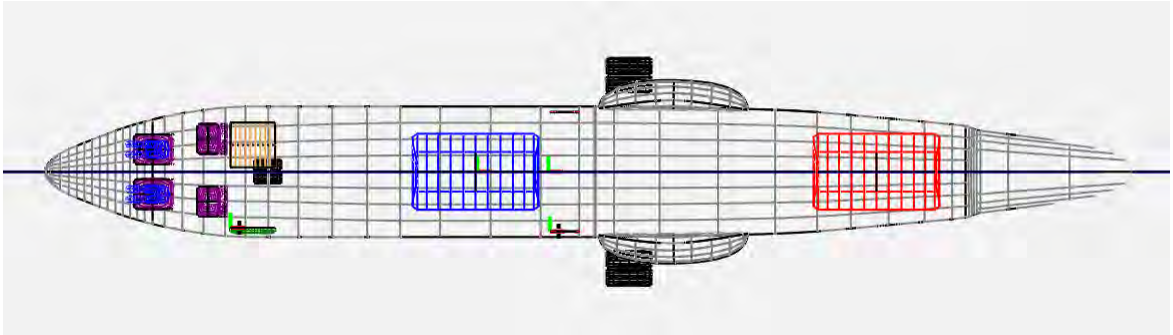

Figure 18 5000 [lb] pound Cargo Layout

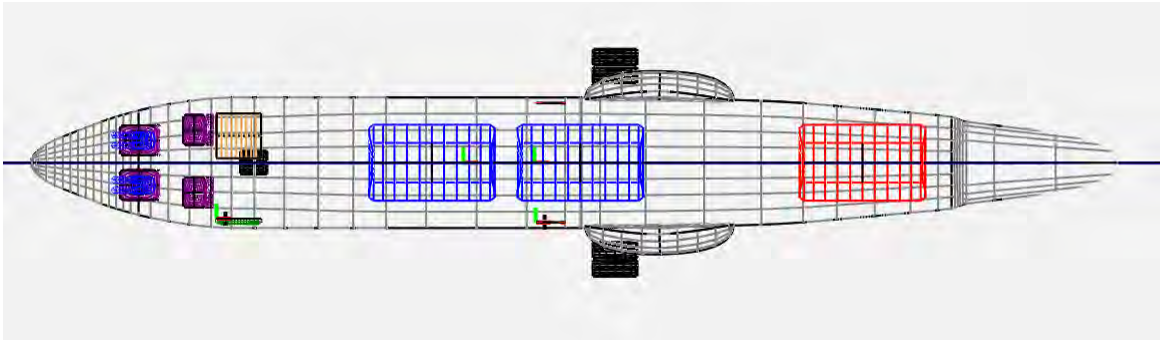

Figure 19 10000 [lb] pound Cargo Layout

From red position to blue positions, rails or rollers can be used to move the container through cargo compartment. Forklifts can be used to put cargo into the fuselage.

4 Chapter 4 – Aerodynamics and Installed Thrust

4.1 Aerodynamics

4.1.1 Aerodynamic Analysis

Once the drawings of MI-1 finished the next step was to analyze it in order to optimize our design. We had used MIT's Open VSP software to draw the plane and using its analysis tool "VSPAero" was a quick and well solution to the problem.

4.1.1.1 Vortex Lattice Method

VSPAero offered two methods of numerical solutions, Panel Method and Vortex Lattice Method. While Panel method is a newer and a more sophisticated way of solving the flow around an aircraft the complex geometry of MI-1 caused it to experience singularities to the point that it was no longer working. Hence, we went for the older but more reliable way of VLM.

VLM transforms the lifting surfaces into infinitely thin vortex sheets, eliminating thickness and viscosity effects. Once the flow field is simulated in this way, pressure distribution can be extracted which in turn will be used to determine aerodynamic forces and moments. As simplistic as it may be, it provides a good starting point to work on for conceptual design.

4.1.2 $C_{L,alpha}$ and $C_{L,max}$ Calculation:

When plotting lift curve of an aircraft two parameters are needed; slope of the lift curve and its maximum value. For a subsonic aircraft, the slope of the lift curve is affected by various parameters such as fuselage lift factor, exposed wing area, reference wing area, aspect ratio, wing sweep, compressibility factor and airfoil efficiency. Lift curve is calculated from the equations of twelfth chapter of the [1]. For this calculations airfoil efficiency taken as 0.95. All sweep values are calculated from Open VSP. Sweeps are calculated at leading edge, $x = 0.3c$ where $(t/c)_{max}$ and $x = 0.25c$. From the fig. 12.8 of the [1] by assuming subsonic high-aspect ratio wing is used. Since leading edge sweep close 0 degree $C_{L,max} \backslash c_{l,max}$=0.9. Exposed wing area and reference wing area are used to correct the fuselage lift (F). Lift curve and its maximum value changes with Mach number.

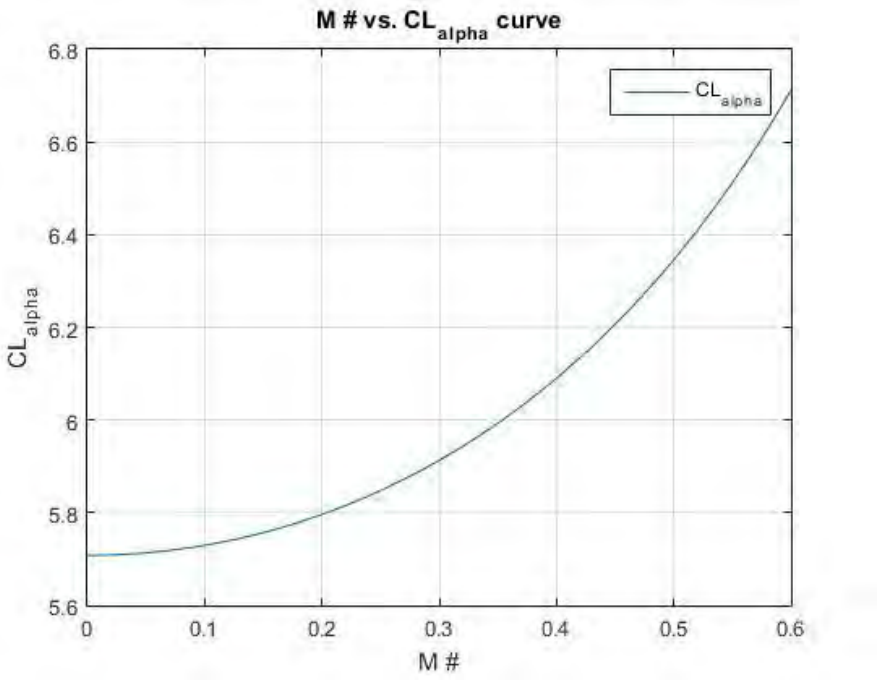

Figure 20 $C_{L,alpha}$ vs Mach number

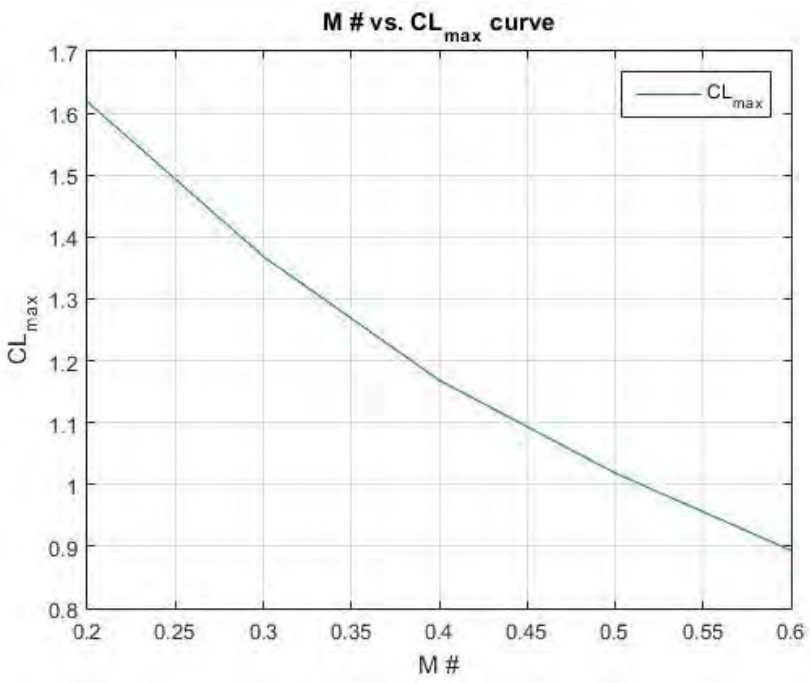

Figure 21 $C_{L,max}$ vs Mach number

Maximum $C_{L,max}$ coefficient is calculated with the leading edge and trailing edge devices. Slotted leading edge flap and fowler flaps assumptions used for equation from the twelfth chapter of the [1]. Therefore, $C_{L,max} = 2.85$ is found.

4.1.3 C_{D0} Calculation:

C_{D0} calculations are found from the equation 12.24 of the [1] but by neglecting the miscellaneous drags which are not necessary for clean configuration. Q is interference factor taken from the fig 12.32 of the [1], Wetted area is taken from the Open VSP. C_f is calculated for the all corresponding Reynolds Number for turbulent flow from equation of 12.27 of [1]. Cut off Reynolds numbers are also calculated (by using smooth paint); however, they are bigger than the classic Reynolds number calculation. So, smaller values are used. Form factor of tail and wing is calculated from equations of 12.30 of the [1]. Thickness ratios and max thickness chords are calculated form the NACA airfoil data. Sweep angle at maximum thickness is also used. For fuselage equation 12.31 of the [1] is used. For external stores equation 12.32 of the [1] is used which is for the engine mount. Also, we have 2 engines, multiply this by 2. Also, we have 2 external equipment to prevent wing tips to go in water. All calculated values are putted into the C_{D0} equations and summed. So, following figures are collected. “f” is the fineness ratio. For protuberance drag, 10% additional parasite drag is added for propeller aircraft.

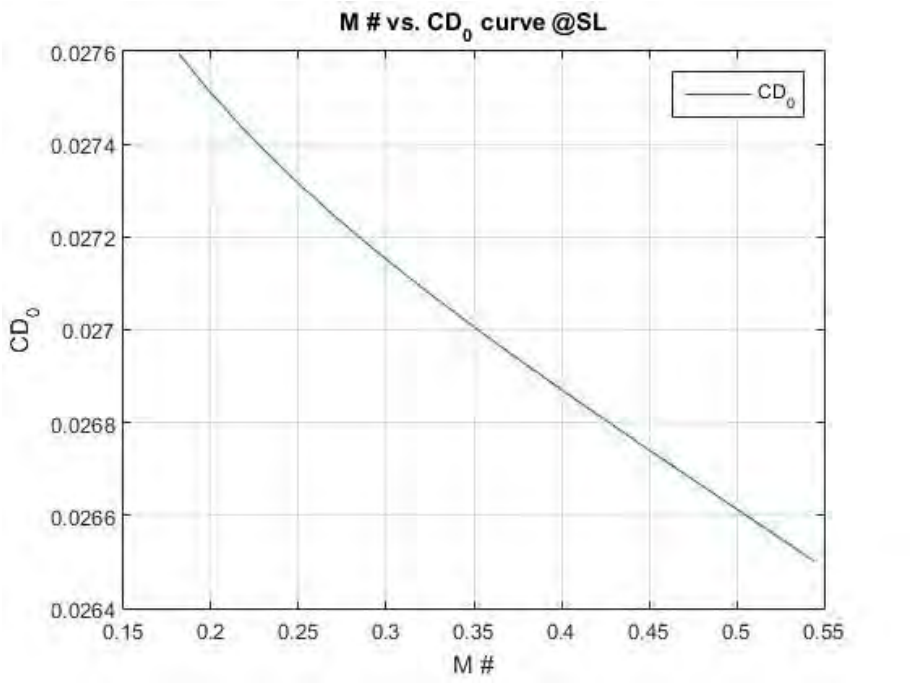

Figure 22 C_{D0} vs Mach number at sea level

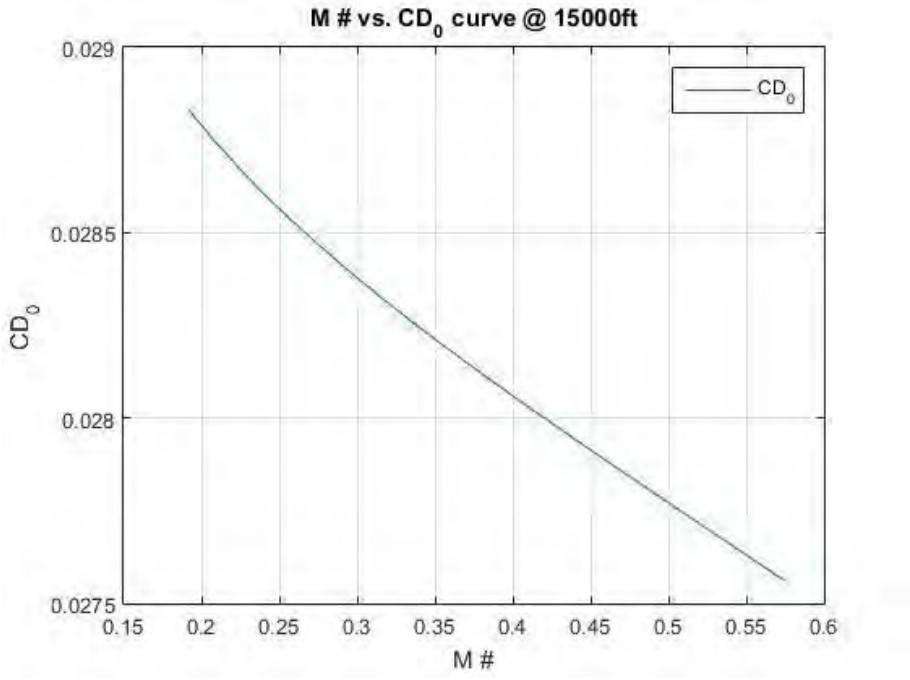

Figure 23 C_{D0} vs Mach number at 15000 ft altitude

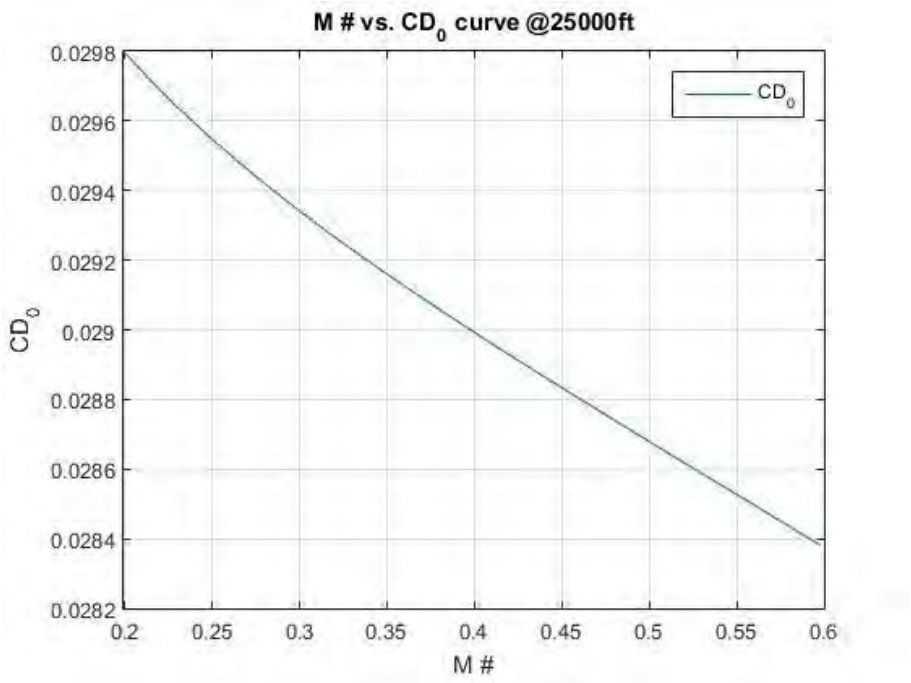

Figure 24 C_{D0} vs Mach number at 25000 ft altitude

The parasite drag coefficient analysis clearly indicates that the efficient flight can be achieved at lower altitudes, as altitude increases drag and due to lower speed of sound at higher altitudes, the same speed is reached at a higher Mach number which also causes the drag to increase.

With 0 sideslip angle and 0.37 Mach number following aerodynamic properties obtained from the Open VSP programs analysis:

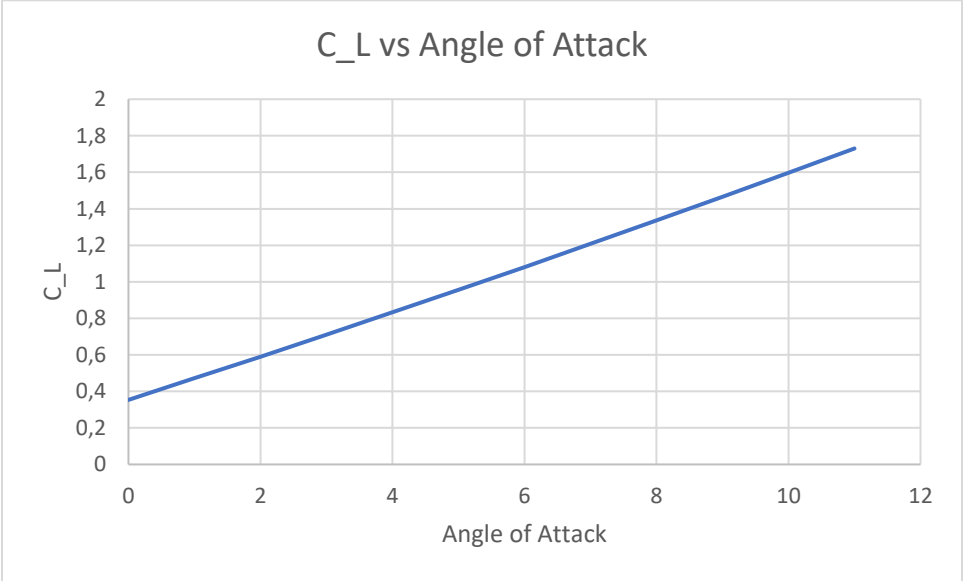

Figure 25 C_L vs Angle of Attack

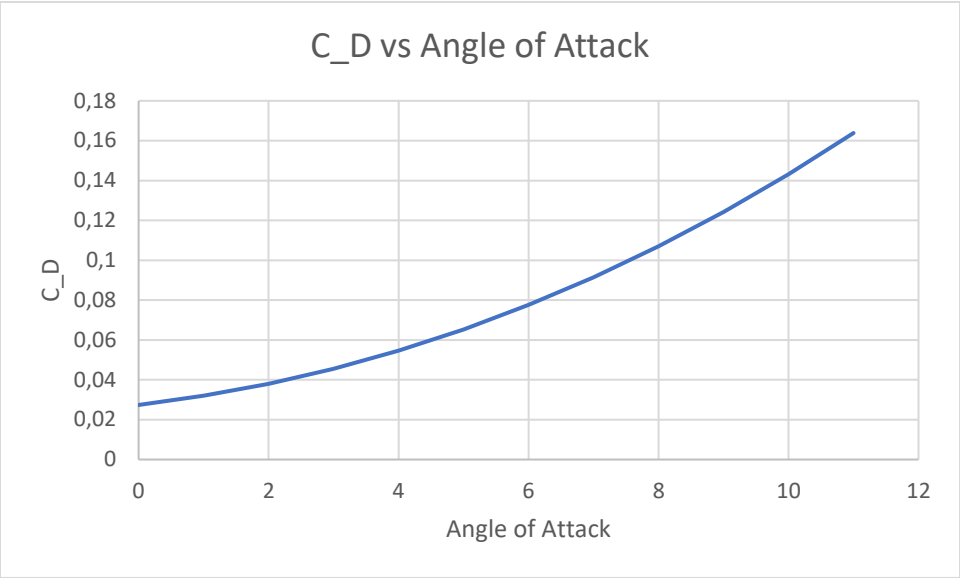

Figure 26 C_D vs Angle of Attack

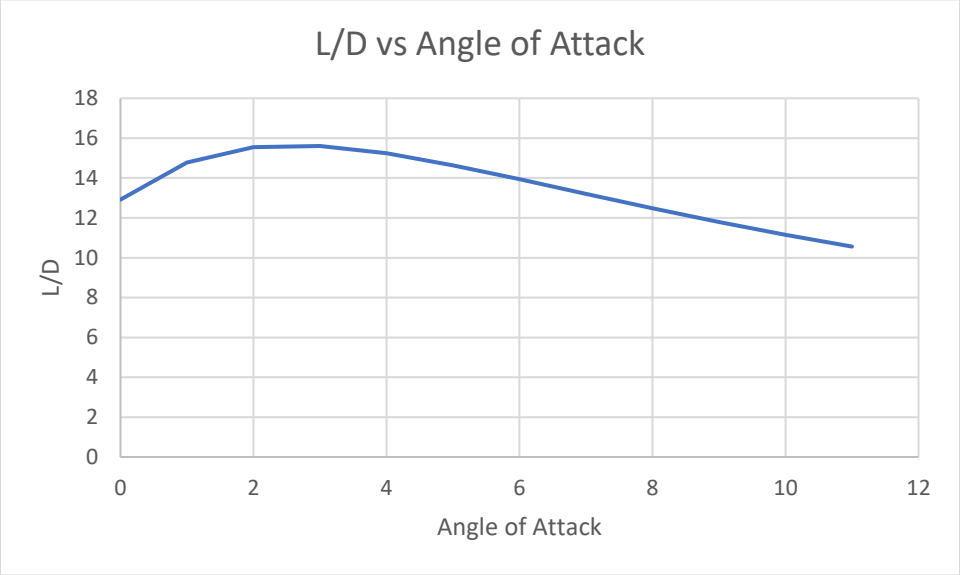

Figure 27 L/D vs Angle of Attack

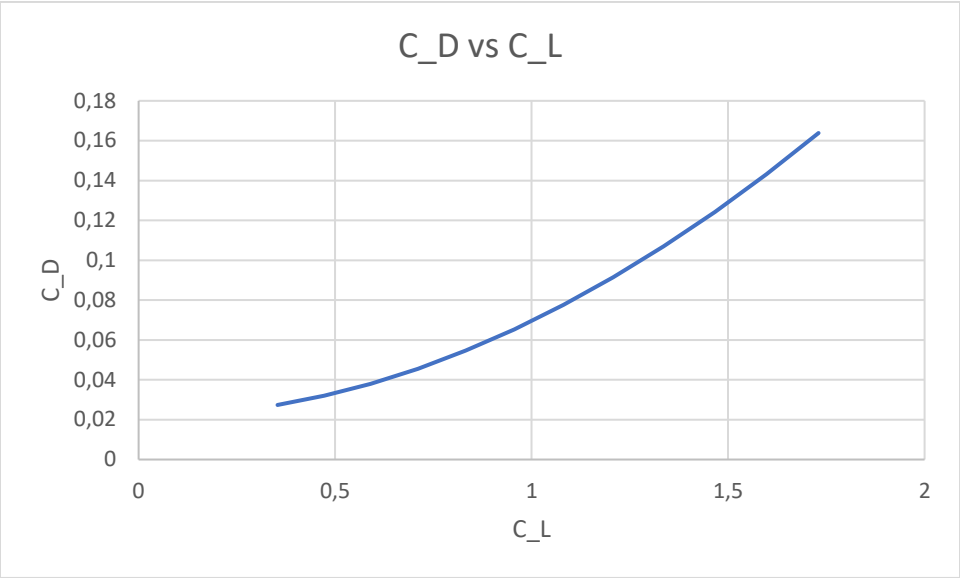

Figure 28 C_D vs C_L

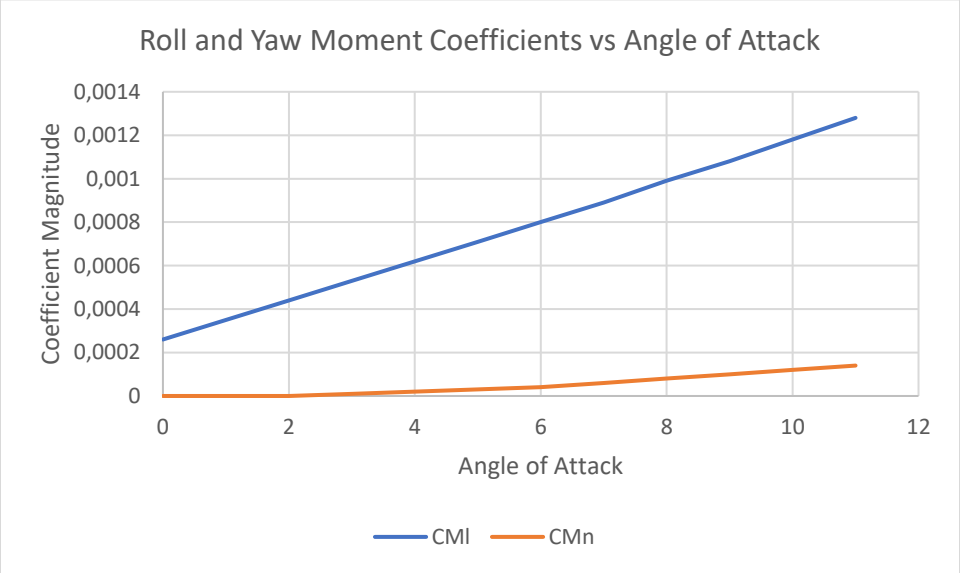

Figure 29 Roll and Yaw Moment vs Angle of Attack

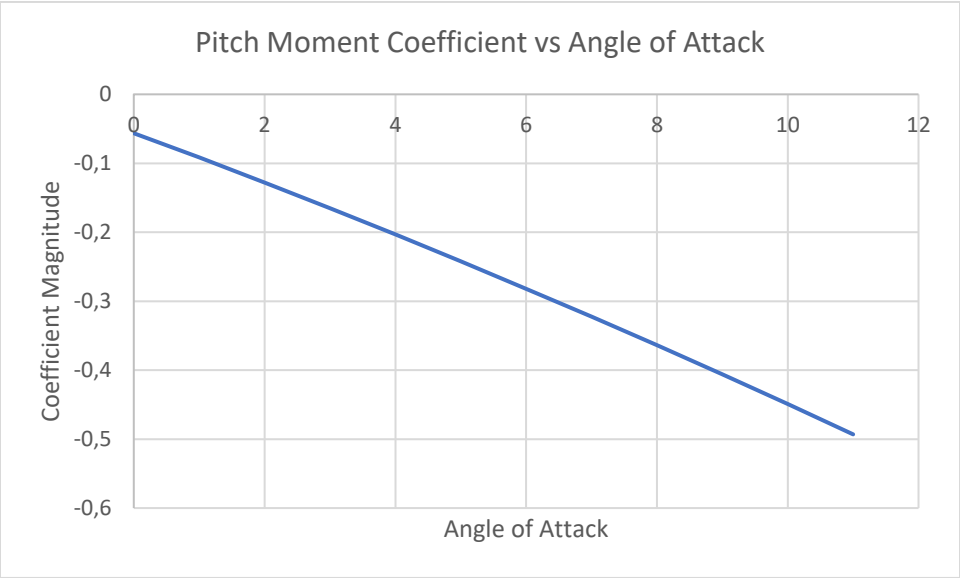

Figure 30 Pitch Moment vs Angle of Attack

vspAERO is additional analysis tool for Open VSP opensource program. It uses Vortex Lattice Method (VLM) to calculate aerodynamic coefficients. Solution neglects viscosity and thickness (infinitely thin aircraft surfaces).

4.1.4 Induced Drag Coefficient:

Induced drag is caused by the produced lift. It is found by multiplying the lift coefficient with the K factor. To find K factor, Oswald efficiency factor should be found. It is found as $e = 0.8247$ by using the equation 12.46 of the [1]. Therefore, $K = 0.0573$. Since Re decreases with altitude it means that the K increases with altitude and thus the induced drag will also increase with altitude.

4.2 Thrust correction

In this part, the objective is to find the uninstalled thrust and the efficiency of the turboprop engine which is referred as a performance mixture of piston-prop engine and jet engine. It is little bit troublesome to find since Mi-1 has a variable pitch engine uses 6 blade-propeller. So, different approaches tried to follow.

One is started with power scale factor and for constant rpm, advance ratio is calculated and corrected for blockage effects. For thrust calculations turboprop uninstalled thrust graph of A.4 of the [1] is digitized and scaled. Installed thrust is calculated with miscellaneous and cooling drags. Also, efficiency of the propeller is assumed to be constant as 0.8 and its corrected for different scrubbing and compressibility influences.

Other methodology is to digitize the efficiency of the 3-blade propeller engine and then interpolate variables to get a function to calculate propulsive efficiency. Variables from fig 13.9 of the [1] are power coefficient, advance ratio and the efficiency. Power coefficient and corrected advance ratio also are in our calculations for propeller and engine which are matched with variables from graph to get efficiency for our corresponding propeller. After interpolation, efficiency is corrected and other losses are calculated as in first approach then

installed thrust is found. Note that our engine is PW150A which can produce over 5000shp with 1020rpm and our propeller is Dowty R408 with diameter 13.5ft. Extracted power found as $P_{ext} = 55.7$.

Blockage effects:

J is the advance ratio and S_c is the front view area of the nacelle. “n” is the rpm and D is the diameter. V is the flight velocity which is calculated for corresponding Mach number and speed of sound, a, at different altitudes. Advance ratio is corrected by using the equations of thirteenth chapter of the [1].

Compressibility

Compressibility effect on propeller efficiency is calculated for the Mach number at the tip of the airfoil by using the equations of thirteenth chapter of the [1].

Scrubbing

Scrubbing effect corresponds to wetted area influenced by the flow behind the propeller. Nacelle and the wing part behind the propeller also, the tail part is included for this effect to be conservative. Normally, tail may not be influenced by propeller because engines are carried on top of wing.

Cooling Drag

Cooling the engines slows down the oncoming air and this generates a drag that must be subtracted from the thrust of the engine at any velocity and altitude. It is found by using the equation 13.18 of the [1].

Miscellaneous Drag

Miscellaneous engine drag includes the drag of the oil cooler, air intake exhaust pipes, and the other parts. It is calculated by using equation 13.19 of the [1].

Installed Thrust

Installed thrust can be found by using the below equation. Note that for higher number of blades, efficiency can be assumed 5 percent less and thrust 5 percent more. The term η_{corr2} is found by using equation 13.17 of the [1].

$$T_{installed} = T_{uninstalled*}\eta_{corr2} - D_{cooling} - D_{misc}$$

4.2.1 Method 1

In this approach, efficiency is accepted as 0.8 as first but it is corrected after. Uninstalled thrust is digitized from the graph and scaled, also it is installed by considering the efficiency and drags.

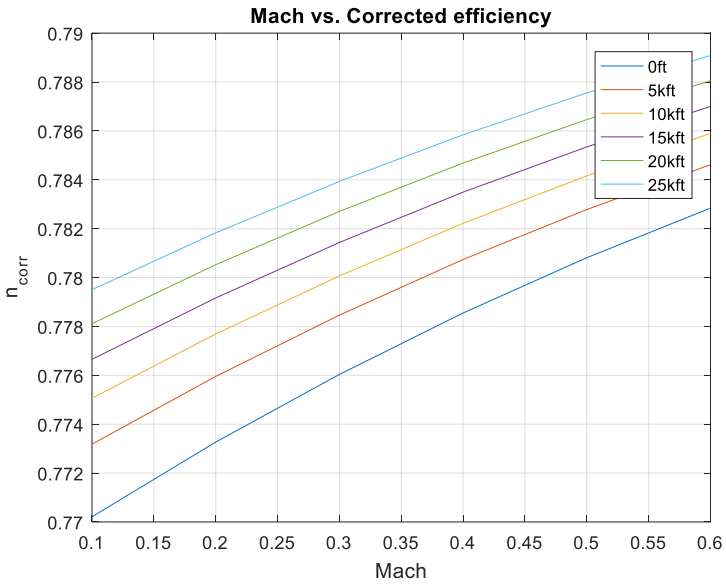

Figure 31 Corrected efficiency vs Mach number at different altitudes

Since the efficiency is accepted as 0.8 at first, efficiency graph does not look like to go zero at the 0 Mach. So, it is not a useful approach. Also, for higher Mach numbers it is not very useful.

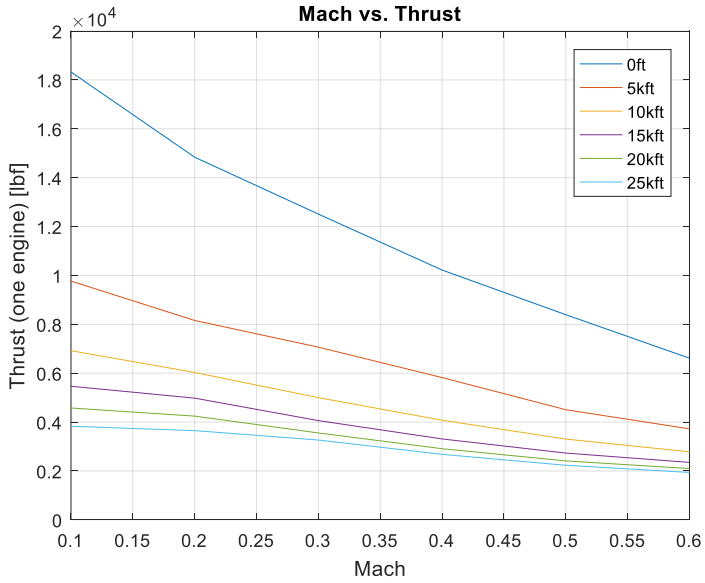

Figure 32 Thrust vs Mach number at different altitudes

Thrust curve is digitized and then corrected and installed so, it is reliable. However, this is even corrected for 3-blade propeller.

4.2.2 Method 2

Efficiency is digitized from corresponding drag by taking values from the different pitch angles.

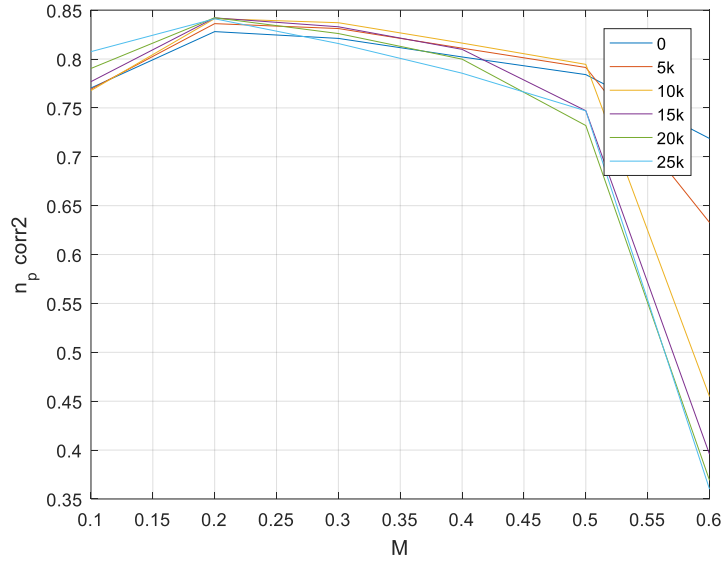

Figure 33 $n_{p,corr2}$ vs Mach number at different altitudes

This efficiency curve has more meaningful alignment by having maximum efficiency Mach number.

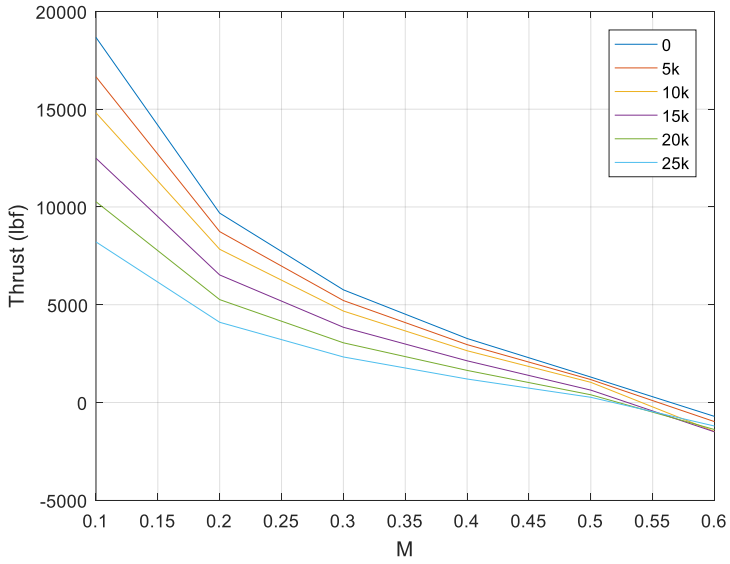

Figure 34 Thrust vs Mach number at different altitudes

Thrust curve has good orientation for 0.1 Mach to 0.3 Mach; however, it has negative thrust at last.

4.2.3 CONCLUSION

Neither of approaches are reliable. Lack of information about propeller geometry does not let us to calculate efficiency in most reliable manner. Also, some found equations that relates advance ratios and propeller efficiency is not used and put into report because of no reference existence. About the results, thrust

digitized from uninstalled thrust curve is reliable by considering efficiency (1st approach); however, 2nd approach and its digitization are not very applicable because of different variable pitch.

5 Chapter 5 – Static Longitudinal Stability

The goal of this part is to evaluate the stability of our craft. This evaluation is done based on the change of stability margin and pitching moment coefficient with respect to Mach number and under different loading configurations. By using the equations of the [1] following results are obtained.

Table 10 Aircraft's Longitudinal Stability Parameters

	Value		**Value**
F	1.28	V_{HT}	0.60
F_{HT}	1.15	$C_{L_{\alpha_{wb}}\text{ at M=0}}$	5.43
K_A	0.11	$h_{n_{wb}}$	0.25
K_λ	1.21		

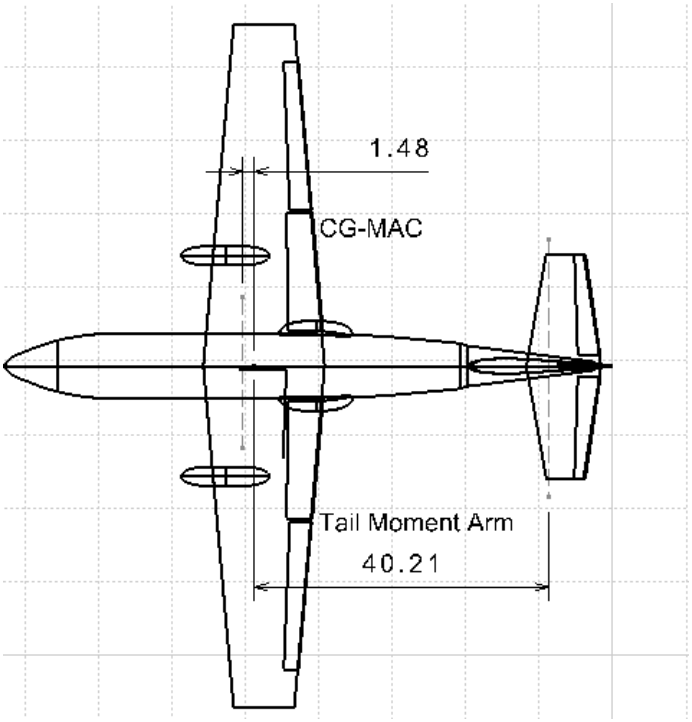

Figure 35 Tail Moment Arm and CG-Neutral Point Locations.

CG and neutral point locations are shown in figure 35. Tail moment arm used in the calculation is also shown.

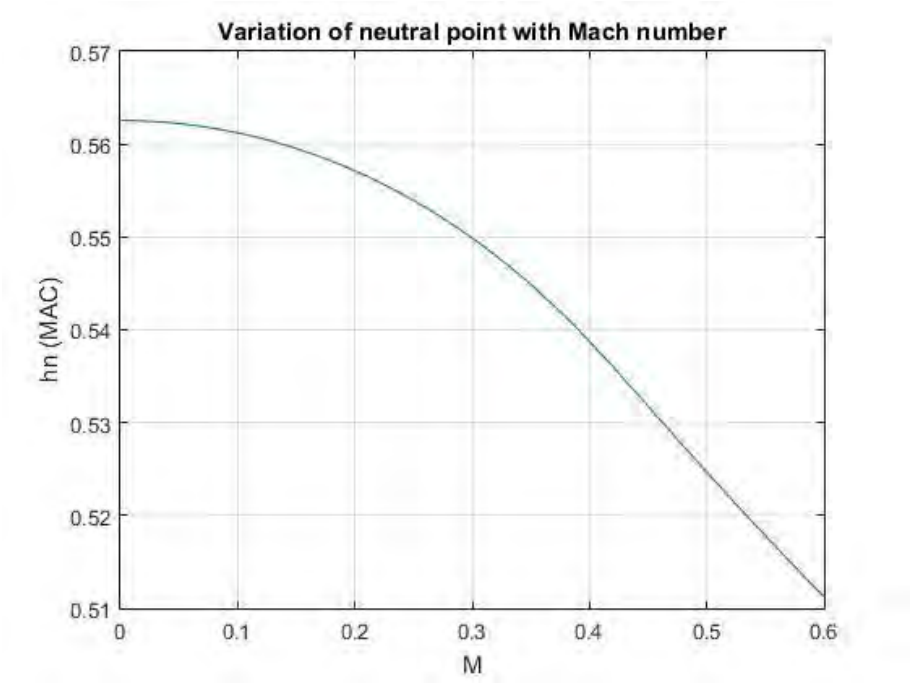

Figure 36 Variation of neutral point with Mach number

Mi-1's designed speed is between 0.3 and 0.35 where it's change from zero velocity is less than 0.02. This is an acceptable change by our estimation since it shouldn't go any faster than 0.35 Mach and initial slope is very low. Variation of neutral point is important because it affects the static margin which is the main scalar to determine the stability and in-turn controllability of the craft. For the graphs above the craft was taken at its worst possible cases of load imbalance where for the passenger mission most forward cg position is for half fuel, full passenger and no passenger cargo configuration and for the most rearward cg position, configuration is for no passenger, full passenger cargo and half fuel situation. For stability, static margin must be negative while a high numerical value would cause it to be too stable, impairing maneuverability.

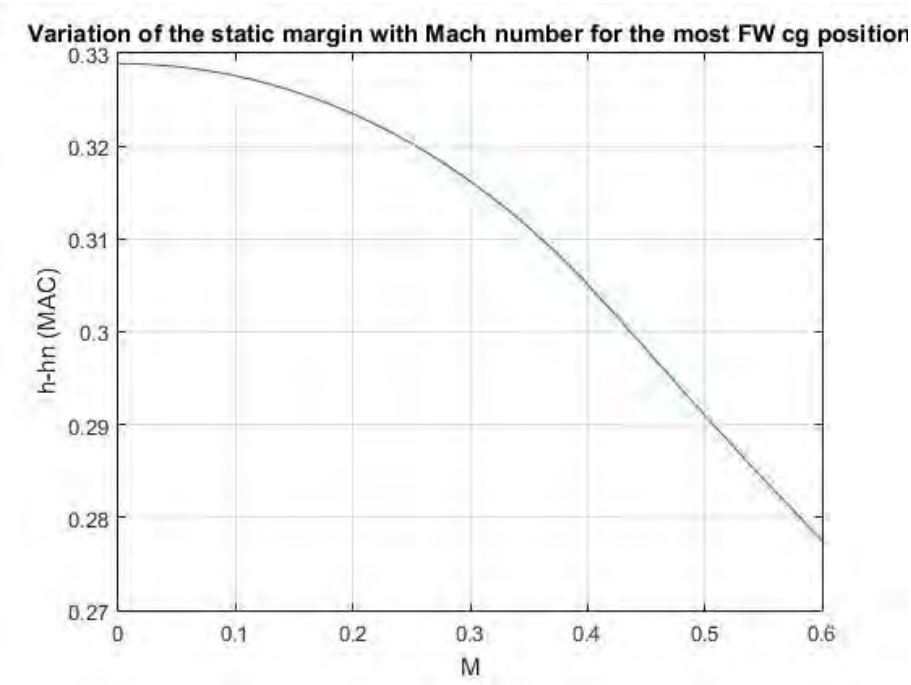

Figure 37 Variation of static margin vs Mach number for the most FW cg position

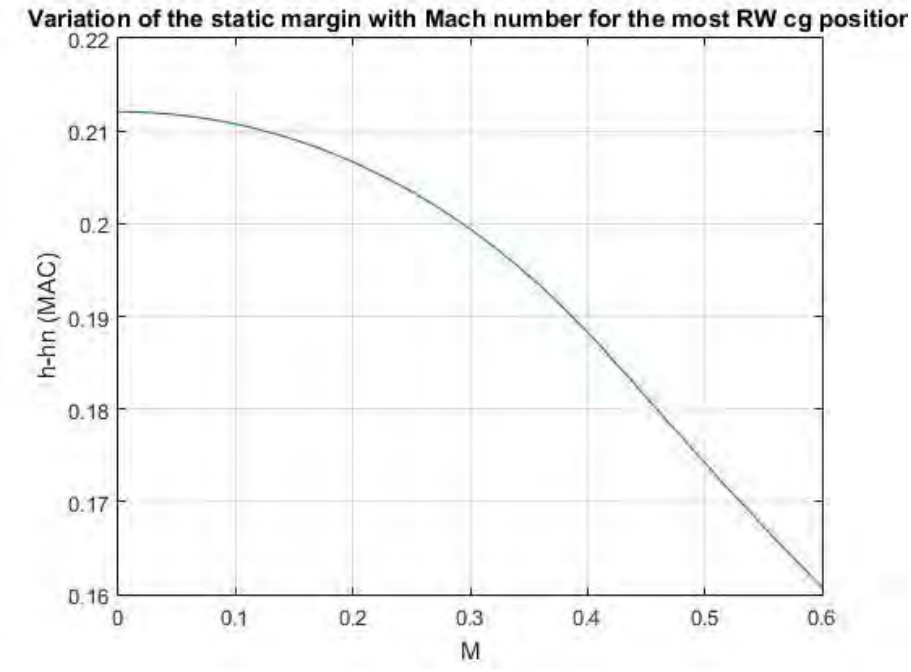

Figure 38 Variation of the static margin vs Mach number for the most RW cg position

The resultant values indicate a stable plane even under worst cases while not impairing maneuverability. The typical values range from 0.05 to 0.4 hence it satisfies those requirements easily.

Lastly the aerodynamic properties of the wing cause a change of pitching moment derivative with respect to angle of attack with change in Mach number. A negative value is required to have a stable craft. In the following section that value is analyzed.

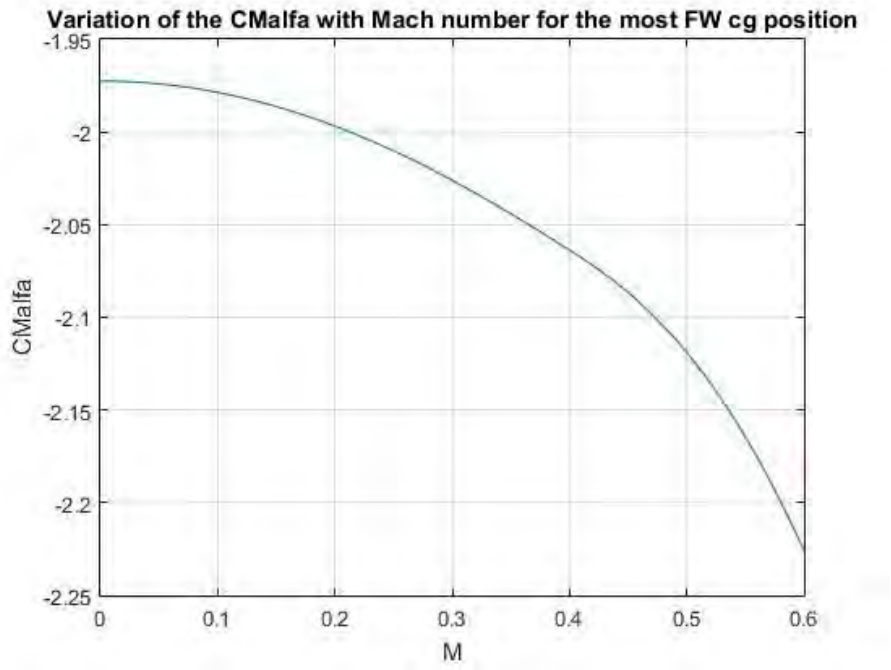

Figure 39 Variation of the $C_{M,\alpha}$ vs Mach number for the most FW cg position

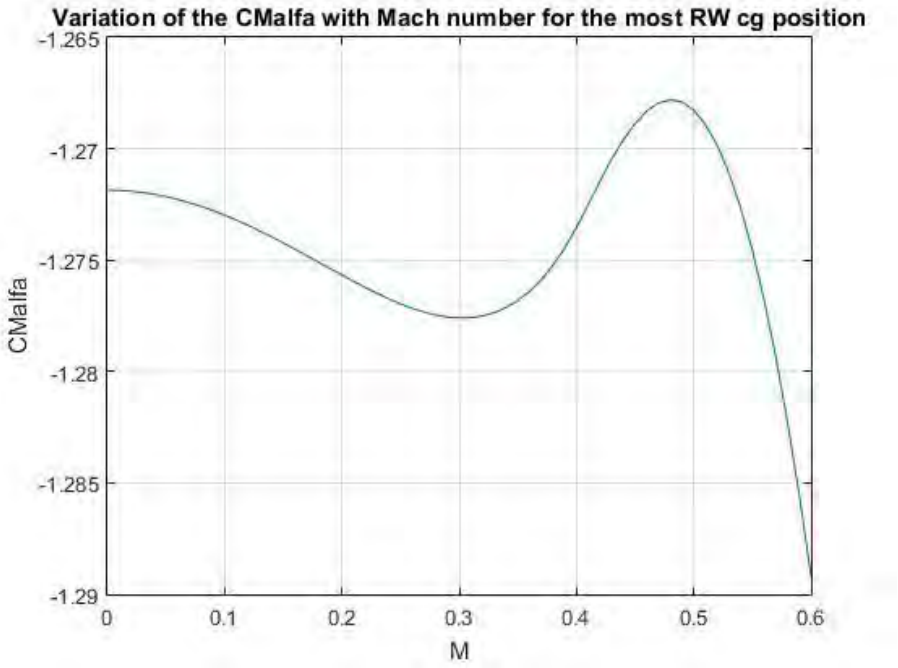

Figure 40 Variation of the $C_{M,\alpha}$ vs Mach number for the most RW cg position

Using the same worst conditions as the last section, we achieve the graphs above. They all indicate negative values which is satisfactory.

6 Chapter 6 – Detailed Empty Weight Calculation

In this part, statistical group weights estimation is calculated. Empty weight, design gross weight is found by considering various parts of aircraft. Equations in fifteenth chapter of the [1] are used. Weight estimation for the Cargo/Transport aircraft relations are used. These equations are based on the statistical data. Hence, for each type aircraft, it should be different. Earlier design parts are used in this part because of the geometric characteristic of the aircraft is needed.

Table 11 Statistical Group Weights

Weights and Ratios	Passenger Mission	Surveillance Mission	Cargo Mission
W_e	31563.08	30645.08	30645.08
W_f	7000.00	7000.00	3500.00
W_{crew}	695.36	1637.97	935.98
$W_{cargo\&payload}$	1463.58	3000.00	5000.00
$W_{passenger}$	7576.16	-	-
W_0	48298.18	42283.05	40081.07
W_{troop}	-	5827.81	-
$W_{0_{troop}}$	-	48110.87	-
W_e/W_0	0.65	0.72	0.76
$W_e/W_{0_{troop}}$	-	0.64	-
W_0/S	42.01	36.78	34.86
$W_{0_{troop}}/S$	-	41.85	-
P	10140	10140	10140
P/W_0	0.21	0.24	0.25
$P/W_{0_{troop}}$	-	0.21	-

7 Chapter 7 – Loads

In this part, the V-n diagram is drawn for sea level. Stall line, structural limit and the gust loads are considered. Cruise speed, maximum speed and dive speed is placed on the V-n diagram.

7.1 Air Loads

7.1.1 Cruise speed, maximum speed and dive speed

For a propeller plane cruise speed is the speed where lift to drag ratio is maximum. It was found approximately as 223 ft/s at sea level. Maximum speed is the speed at which the maximum power available is equal to the power consumed during the flight. It was found approximately as 484 ft/s at sea level. Dive speed is found by multiplying the cruise speed by 1.5. It is found as 580 ft/s.

7.1.2 Stall line

Stall line is found by calculating the maximum possible load factor using the maximum lift coefficient. For negative load factors the minimum lift coefficient is used in the equation.

7.1.3 1-g stall speed

It is the speed at which 1-g load factor line crosses the stall line. It is found as 137 ft/s.

7.1.4 Corner speed

It is the speed at which the limit load factor line crosses the stall line. It is found as 306 ft/s.

7.1.5 Limit load factor line

Positive limit load factor is selected as 3.5 and negative limit load factor is selected as 1.5. Positive limit load factor is corrected to 5 after the addition of gust loads into the consideration.

7.1.6 Addition of gust loads

At first, mass ratio is calculated, then gust load alleviation factor is calculated. Standard vertical gust is taken as 30 ft/s up to the cruise speed and it was decreased linearly to 15 ft/s at dive speed. Using the standard vertical gust and the gust alleviation factor, the gust velocity is calculated. Using the gust velocity, the extra load factor due to gust is calculated.

7.1.7 Result:

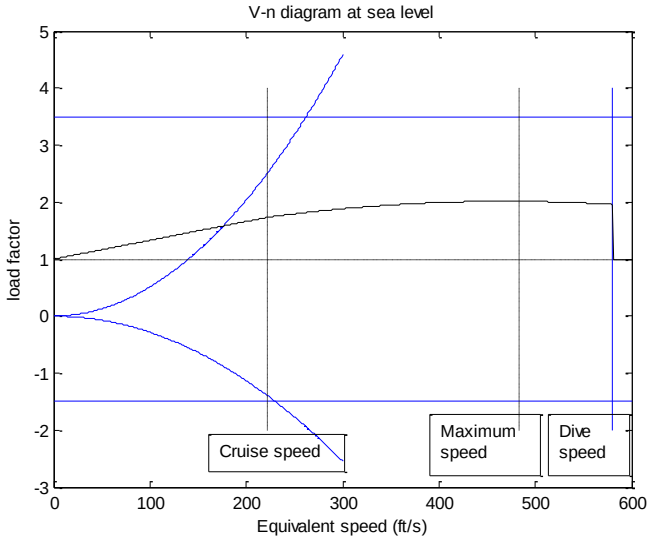

Figure 41 V-n diagram of the aircraft at the sea level

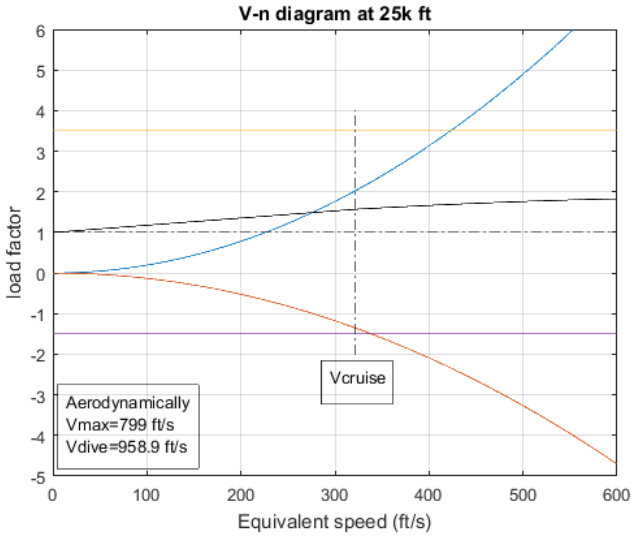

Figure 42 V-n diagram at 25,000 altitude

7.2 Water Load

Hull and main float load factors for landing are found according to the FAA regulations. Step landing case:

$$n_w = \frac{C_1 V_{S0}^2}{\left(\tan^{\frac{3}{2}}\beta\right) W^{\frac{1}{3}}}$$

Original formula is as follows and it includes V_{S0^2} term, in this report it is treated as V_{S0}^2 because, load factor cannot be less than 2.33 according to FAA regulations. C_1 value change or stated change of V_{S0^2} gets load factor to meaningful value. Bow and stern landing cases:

$$n_w = \frac{C_1 V_{S0}^2}{\left(\tan^{\frac{3}{2}}\beta\right) W^{\frac{1}{3}}} \frac{K_1}{(1 + r_x^2)^{\frac{2}{3}}}$$

$C_1 = 0.012$ is empirical seaplane operations factor. V_{S0} is the seaplane stalling speed in knots in our case: $V_{S0} = 128.7 ft/s$ for 45000 lb and flaps extended. $V_{S0} = 76.6\ knots.\beta$ is deadrise angle at longitudinal station.

W is the seaplane design landing weight in pounds? $W = 45000lb$ for passenger mission with design configuration: 39 passengers. Taken conservative, it would be less. K_1 is the empirical hull station weighing factor. This is based on figure from the [1]. r_x is the ratio of distance between hull longitudinal station and CG location according to hull reference axis.

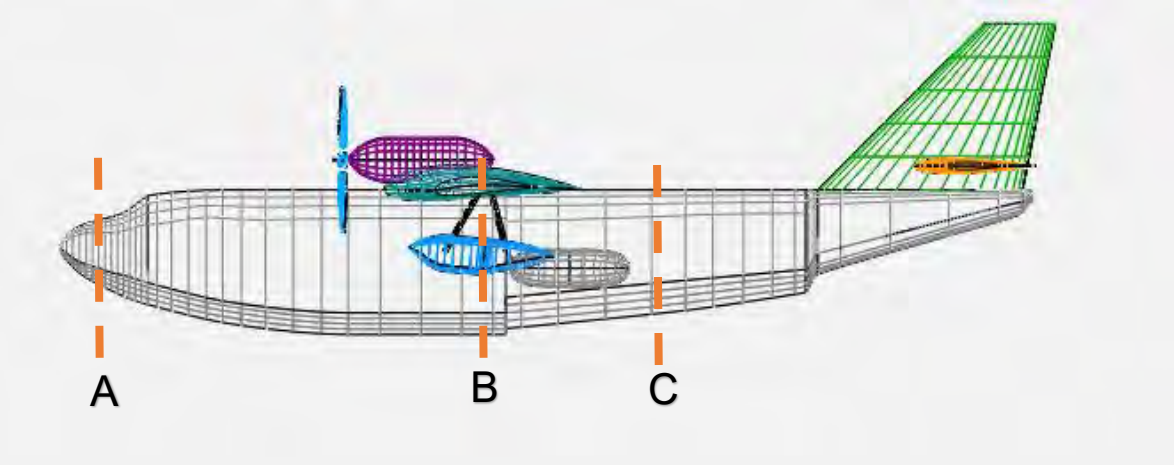

Figure 43 Hull longitudinal station and CG location of the aircraft

Bow	Step	Stern
A	B	C
$x = 4.5'$	$x = 37.05'$	$, x = 52'$

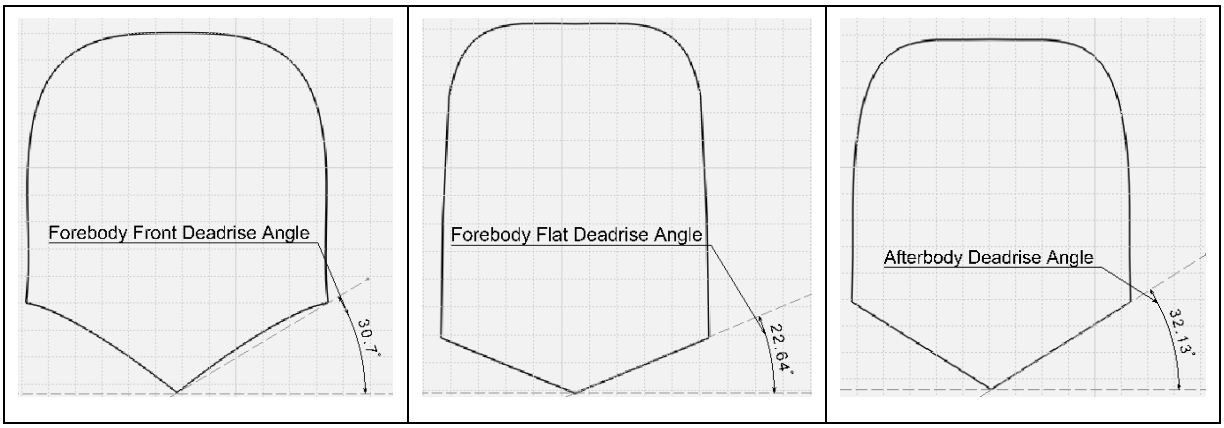

K_1 and β chosen as following table and results added at last row.

Station	Bow	Step	Stern
$\beta\ in\ degrees$	30.70	22.64	32.13
K_1	1.40	0.38	0.75
r_x	0.14	1.10	1.54
n_w	5.5	3.98	1.32

According to results in the above table, landing must be done by considering load factors. Stern landing is the best configuration for landing. Otherwise, landing may cause nose down moment and crash.

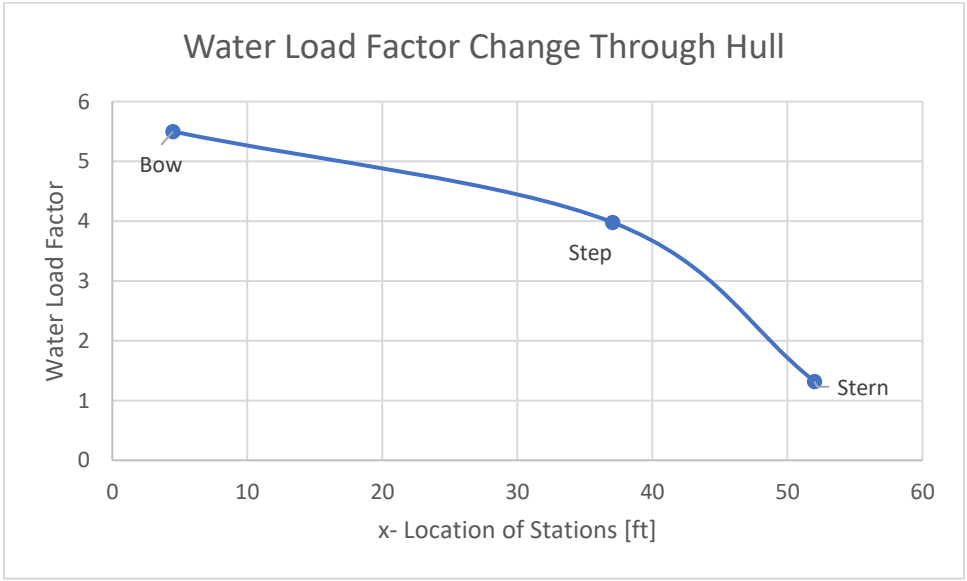

Figure 44 Water Load Factor vs x-location of Stations

8 Performance

Table 12 Performance values of the design

Performance	
Cruise speed at 25000 ft (knots)	198,03
Cruise speed at 30000 ft (knots)	216,60
Cruise speed at sea level (knots)	132,60
Best endurance speed at sea level (knots)	100,80
Takeoff distance [ft]	1374,00
Landing distance [ft]	1123,80
Water takeoff distance [ft]	1460,90
Water landing distance [ft]	1173,00
Range [nmi]	988,90
Endurance [h]	9,65

As it can be seen from the Table 12, some of the performance requirements cannot be met. Range and endurance requirements are calculated based on the specific fuel consumption values of the existing PW150A engine. A future engine may have a better efficiency. Another solution to this problem is carrying more fuel. There is enough space in the wings to carry the extra fuel needed. Carrying 200 [lb] more fuel in the passenger mission and 300 lb more fuel in the endurance mission will resolve the problem. However, this may increase the maximum takeoff weight and affect the other performance values, specifically the landing and takeoff distances. It may also effect the position of the cg. Thus, a new design cycle should be done to satisfy the requirements with a minimum weight.

Another important requirement was the fuel burnt per passenger. It had to be better than a similar aircraft on a similar mission length. Fuel consumption of Bombardier 415 was found per 30 passengers it carries. This value was compared to the value of Mi-1

Table 13 Fuel burn per passenger

	Fuel burnt per passenger(kg/km)
Mi-1	0,0502
CL-415	0,0706

Mi-1 is 29 percent better than CL-415.

8.1 Take-off, Landing Performances

For the calculation of the takeoff and landing distances Chapters 6.7 and 6.8 of [14] are used.

The following values are used for the friction coefficients:

Table 14 Friction coefficient values

Friction coefficient		
Surface	takeoff	landing
dry pavement	0,05	0,5
dirt	0,04	0,3
grass	0,08	0,2
metal mat	0,03	0,2
gravel	0,05	0,3
asphalt	0,05	0,5
concrete	0,05	0,5
water	0,15	0,15

Takeoff and landing distances are shown for the listed cases.

Table 15 Takeoff and landing distances

	Takeoff distance (ft)	Landing distance (ft)
250 nmi 20 passenger sea level		
dry pavement	1374	1124
dirt	1367	1148
grass	1397	1164
metal mat	1360	1164
gravel	1374	1148
asphalt	1374	1124
concrete	1374	1124
water	1461	1173
250 nmi 20 passenger 5000 ft		
dry pavement	1575	1231
water	1695	1294
1000 nmi 39 passenger sea level		
dry pavement	1588	1153
water	1730	1207
Cargo 500 nmi 5000 lb sea level		
dry pavement	1414	1105
water	1511	1151
Surveillance 10 h sea level		
dry pavement	1588	1095
water	1730	1139

9 Chapter 9 – Cost Estimation

Determining the cost of production is not detached from the targeted market as all initial investments will be made according to the expected market demand. Hence, we will start analysis at the market.

9.1 Market Potential

Using the background and the properties of our design we decided to place it in the same market with small airliners. Then we searched for companies that worked around islands or usable water bodies that would be interested in the design. For the passenger category, this search yielded a number around 130 worldwide. Since our plane is a multi-mission one a market penetration of 70% is chosen with the assumption that an average of 2 planes will be bought per company. Resulting in a total of 182 planes. Using this information, we extrapolated decreasingly to estimate cargo and surveillance sales which resulted in 112 and 42 planes respectively.

9.2 Production Cost

Now that we have an expected market demand, we can start estimating the production cost. Production cost consist of engineering, development, tool, quality control and manufacturing, flight test costs as well as engine, avionics and interior decoration costs. In order to estimate the final cost, RAND Corporation's DAPCA IV model is used which incorporates working hours, wrap rates and additional standalone costs.

9.2.1 Non-recurring Costs

Non-recurring costs are one-time expenses like design, tooling, facilities, air and ground tests and certification. Breaking apart the DAPCA model we can find each of them. Although some of the engineering work is spread throughout the production time, exemplary calculation yielded a negligible partition to production time for the assumed order quantity. It should be noted that 3 aircrafts are assumed to be used for certification.

9.2.2 Flyaway Cost

This is the cost that must be paid for every batch of production. This includes the tooling, manufacturing materials, engine expenses and avionics. During these calculations avionics spending is found by empty weight relations while engine is a chosen model and has a set price, the engine expense is the cost of two engines required per each aircraft.

Table 16 Production cost for each mission

Category\Class	Passenger(182)	Cargo(112)	Surveillance(42)	Factor
Engineering	7.9263	7.2469	6.1679	1e+08
Tooling	5.2533	4.5556	3.5246	1e+08
Quality Control	2.5188	1.0324	0.9681	1e+06
Flight Testing	1.4411	1.4319	1.3158	1e+06
Manufacturing	1.7185	1.2326	0.6605	1e+08
Manufacturing Materials	7.6364	5.0683	2.325	1e+08
Development	1.3221	1.3275	1.3158	1e+08
Engine Expense	4.4017	4.4017	4.4017	1e+06
Avionics	1.89378	1.89378	1.89378	1e+08
Flyaway costs	0.6645	0.7113	1.2344	1e+07
Non-Recurring Cost	**3.1701**	**2.5470**	**1.7628**	**1e+09**
RDT&E + Flyaway Cost	**4.6585**	**3.8323**	**2.4617**	**1e+09**
A/C Sale price (%15 profit)	**2.9436**	**3.9350**	**6.7404**	**1e+07**

9.2.3 Material Selection

All throughout the design process the discussion over the materials was a fiery topic with one side emphasizing over the performance benefits while the other was focused on the cost and availability of the alternatives. The materials in question was composites and aluminum respectively. In the end when it was found that the requirements can be met without the composite manufacturing, it was a matter of optimization to choose the material. Using the DAPCA IV model and interpolating a fudge factor, the increase in both the production and the maintenance for a composite plane deemed it as an overdesign. Hence MI-1 is an aluminum seaplane.

The only exception to this is the landing gear struts where high load factors, including impulse load is an expected risk. Hence to make MI-1 durable against it they are chosen as steel.

9.3 Operating Cost

Aircraft operating cost is the yearly expense that the operator will have to endure in order to safely continue operating the aircraft. These expenses must cover fuel consumption, tires and other materials, maintenance labor fees and finally crew salaries. Continuing to use the DAPCA IV model we can estimate these as given in the table below.

Table 17 Operating cost for each mission

Category\Class	Passenger	Cargo	Surveillance	Factor
Fuel Costs	2.5571	2.5571	1.1591	1e+06
Material costs	3.6246	4.5826	5.4351	1e+08
Crew Salary per year	2.4777	3.3036	4.0765	1e+06
Maintenance Labor Per year	38.22	38.22	26.95	1e+05
Total Cost Per year	**3.7132**	**4.6794**	**5.5144**	**1e+08**

DAPCA IV uses block hours to estimate maintenance, crew and material costs. Considering MI-1's payload capability and arrangement we found that an estimate of half an hour ground preparation and unload time would be appropriate. This would make the block hours as:

Category\Class	Passenger	Cargo	Surveillance
Block Hours	6	6	11
Block Hours per Year	3900	3900	2750

At the end of this analysis we have an estimate of the expected production price and the yearly operating cost for MI-1.

10 Chapter 10 – Trade Studies

At this point, a trade study was done and the lightest aircraft that satisfies all of the major requirements was found. The requirements that were considered are: range of the passenger mission, endurance of the surveillance mission, takeoff and landing distances from land and water and cruise speed.

The aircraft was optimized in terms of power and wing area. The change in the weight of the aircraft was found in terms of the power and the wing area. Two different engines are used to calculate the power variation. These engines are Pratt and Whitney PW127 and PW150A. Three different wing area values are used to estimate the variation of the weight in terms of wing loading. Total of 6 points are used to make an optimization. These six points are curve fitted to estimate the weight of the aircraft out of the estimated points. Then, performance of the aircraft is calculated and checked if it meets the requirements. The critical points which satisfy the requirements exactly are plotted in a graph as a line and the area where all of the requirements are met is found. The optimum point is found and shown on the graph.

The tables where the requirements are shown are given below.

Table 18 Performance of the aircraft when PW127 engines are used

Performance								
Wing area (ft^2)	MTOW (lb)	Range (nmi)	Endurance (h)	Landing distance (ft)	Takeoff distance (ft)	Sea landing distance (ft)	Sea takeoff distance (ft)	Cruise speed at 25000 feet (knots)
700	42536	1148,4	9,34	1531,3	2644,7	2338,4	3382,8	236,8
750	42789	1144,3	9,58	1466,5	2467,4	2229,5	3109,1	229,5
800	43042	1139,8	9,81	1410	2316,1	2134	2880,6	222,8
850	43295	1135,1	10,03	1360,2	2185,4	2049,5	2687,2	216,8
900	43548	1130,2	10,22	1315,9	2071,6	1974,2	2521,6	211,3
950	43801	1125,1	10,41	1276,3	1971,5	1906,6	2378,3	206,3
1000	44055	1119,8	10,59	1240,8	1882,9	1845,7	2253,2	201,6
1050	44308	1114,4	10,75	1208,6	1803,9	1790,5	2143,1	197,3
1100	44561	1109	10,91	1179,4	1733,1	1740,1	2045,4	193,4
1150	44814	1103,4	11,05	1152,8	1669,1	1694,1	1958,4	189,6
1200	45067	1097,8	11,19	1128,3	1611,2	1651,8	1880,2	186,2
1250	45320	1092,2	11,32	1105,9	1558,5	1612,8	1809,7	182,9
1300	45573	1086,5	11,44	1085,2	1510,3	1576,8	1745,8	179,9
1350	45827	1080,8	11,55	1066	1466	1543,3	1687,6	177,0
1400	46080	1075,1	11,66	1048,2	1425,3	1512,2	1634,3	174,3

Table 19 Performance of the aircraft when PW150A engines are used

Performance								
Wing area (ft^2)	MTOW (lb)	Range (nmi)	Endurance (h)	Landing distance (ft)	Takeoff distance (ft)	Sea landing distance (ft)	Sea takeoff distance (ft)	Cruise speed at 25000 feet (knots)
700	45671,98	1030,3	8,2018	1482,2	2028,8	1574,4	2229,8	268,4072
750	45995,55	1025,8	8,4016	1421,4	1914,9	1505,8	2092,9	260,2229
800	46312,12	1021,3	8,5888	1368,2	1816,1	1445,9	1975,3	252,8253
850	46621,69	1016,6	8,7648	1321,2	1729,7	1393,2	1873,2	246,0950
900	46924,26	1011,9	8,9308	1279,4	1653,4	1346,3	1783,6	239,9362
950	47219,83	1007,2	9,0879	1241,9	1585,5	1304,4	1704,4	234,2711
1000	47508,4	1002,5	9,2372	1208,1	1524,5	1266,7	1633,7	229,0359
1050	47789,97	997,9	9,3794	1177,4	1469,5	1232,6	1570,3	224,1775
1100	48064,54	993,4	9,5154	1149,4	1419,6	1201,5	1513	219,6516
1150	48332,11	988,9	9,6457	1123,8	1374	1173	1460,9	215,4206
1200	48592,68	984,6	9,7711	1100,2	1332,2	1146,9	1413,3	211,4526
1250	48846,25	980,4	9,8919	1078,4	1293,7	1122,8	1369,6	207,7203
1300	49092,82	976,3	10,0088	1058,2	1258,1	1100,5	1329,4	204,1999
1350	49332,39	972,3	10,1221	1039,5	1225	1079,8	1292,1	200,8711
1400	49564,96	968,4	10,2322	1021,9	1194,2	1060,5	1257,6	197,7159

The graph that shows the lines of the requirements, the design point and the optimum points are shown below.

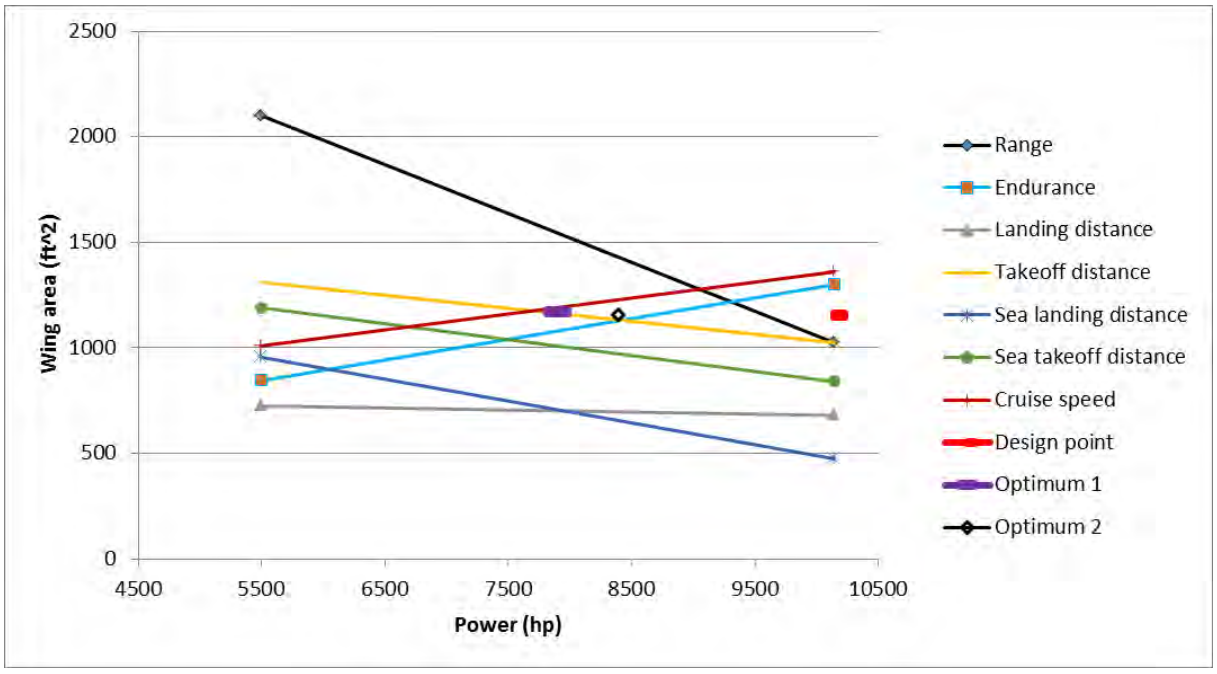

Figure 45 Design point and optimum points

The area where the cruise speed, range, endurance and takeoff distance forms a tetragon is the area in which all of the requirements are met.

There were two possible optimums on the graph. The weight was calculated for both of the points. Optimum 1 point is the point which gives the minimum weight. The values at the design point and the optimum point are shown in the table below.

Table 20 Values at the design point and optimum point

	Design point	Optimum point
Power (hp)	10140	7900
Wing area (ft^2)	1150	1170
MTOW (lb)	48332	46750

An engine which has a power rating of around 4000 hp and a similar power to weight ratio has to be used. There is no such engine available at the market today. However, there may be in the future.

11 Chapter 11 – Aircraft Specifications

11.1 Flight Desk Design

An optimized flight desk design must provide a wide range of information in a compact manner that can enable the pilots to both acquire and respond to different circumstances. The most common and modern way of this is to have digital cockpit configuration. MI-1 will follow the path of Boeing 787 Dreamliner while incorporating extra options to the pilots in terms of information since it is an amphibious aircraft and will have more environmental hazards.

This configuration provides both pilots with the ability to cycle through all flight instruments while also having the ability to warn them about errors, malfunctions and warnings using color-coded lights. In addition to automated warning systems the flight crew will have vision of the interior and the exterior of the airplane through cameras placed at key locations inside the cabin and at wide view angles like the tail fin tip and wing leading edges so that the crew can position and operate the aircraft without the need of a ground crew. This aided by the integrated GPS will make the pilots always aware of their surroundings and position.

Physically the flight desk will consist of three major panels in front of the pilots. The side panels will be symmetric and have 4 touchscreen 10-inch to 13-inch in diamond formation with the center panel for extra buttons such as quick screen changes.

Center panel will have 2 large screens primarily dedicated to air traffic control and communication which will also blend radar data with GPS data to achieve the aforementioned sense of location. Below and behind this panel will have the throttle, flap and trim adjusters available to both pilots.

Overall the flight desk will be designed both for aesthetics and utility with a symmetric design and modern quick response electronic interfaces.

11.2 Conclusion

In this report, the conceptual design of the multipurpose amphibian airplane MI-1 was done. After thorough analysis and competitor study MI-1 has successfully achieved mandatory requirements in every mission category. However, like every design further optimization can and will be done to the design process in the preliminary design phase.

Throughout this design different ways of iterative design methods and optimizations were incorporated with the goal of making the most affordable and reliable aircraft capable of reaching the mandatory requirements and when possible even more. MI-1 is a one of a kind aircraft which is why it will have an impact on the medium airliner market along shores and settlements limited by short runways. Its capabilities are estimated based on physical formulas and relations filled with the experiences of the golden age of flight.

12 References

[1] D. Raymer, Aircraft Design: A Conceptual Approach, AIAA, 1992.

[2] [Online]. Available: http://www.environment.gov.sk.ca/Default.aspx?DN=06f4df9e-a7a4-4923-9e51-d50031e9dca1. [Accessed 10 5 2017].

[3] [Online]. Available: http://www.dornierseawings.com/specifications.html. [Accessed 10 5 2017].

[4] [Online]. Available: http://www.militaryfactory.com/aircraft/detail.asp?aircraft_id=1253. [Accessed 10 5 2017].

[5] [Online]. Available: https://www.aircraftcompare.com/helicopter-airplane/Bombardier-415/87. [Accessed 10 5 2017].

[6] [Online]. Available: http://www.719skvadron.no/dhc6/dhc6-spec.htm. [Accessed 10 5 2017].

[7] [Online]. Available: http://www.militaryfactory.com/aircraft/detail.asp?aircraft_id=1254. [Accessed 10 5 2017].

[8] "engineeringtoolbox," [Online]. Available: http://www.engineeringtoolbox.com/standard-atmosphere-d_604.html. [Accessed 08 05 2017].

[9] "Purdue School of Aeronautics and Astronautics," AlliedSignal Aerospace , [Online]. Available: https://engineering.purdue.edu/~propulsi/propulsion/jets/tprops/pw100.html. [Accessed 10 5 2017].

[10] B. D. a. J. A.G. Smith, "Water and Air Performance of Seaplane Hulls as affected by Fairing and Fineness Ratio," London: Her Majesty's Stationery Office, 1954.

[11] S. Gudmundsson, General Aviation, Butterworth-Heinemann, 2014.

[12 2009. [Online]. Available: http://adl.stanford.edu/sandbox/groups/aa241x/wiki/e054d/attachments/31ca0/performanceanddrag.pdf?sessionID=2db6d225d415d299941c2168906e6421a8cd8152. [Accessed 9 5 2017].

[13 [Online]. Available: https://www.ecfr.gov/graphics/pdfs/ec28se91.056.pdf. [Accessed 10 5 2017].

[14 J. John D. Anderson, aircraft performance and design, Singapore: McGraw-Hill Book Co, 1999.